ELSEVIER

Mutation Research 417 (1998) 65–73

MR
Genetic Toxicology and Environmental Mutagenesis

Molecular analysis of mutations induced by acrolein in human fibroblast cells using *supF* shuttle vector plasmids

Masanobu Kawanishi [a,c], Tomonari Matsuda [a], Aki Nakayama [b], Hiraku Takebe [c], Saburo Matsui [a], Takashi Yagi [c,*]

[a] *Research Center for Environmental Quality Control, Kyoto University, 1-2 Yumihama, Otsu, Shiga 520-0811, Japan*
[b] *Department of Environmental Engineering, Graduate School of Engineering, Sakyo-ku, Kyoto 606-8501, Japan*
[c] *Department of Radiation Genetics, Faculty of Medicine, Kyoto University, Sakyo-ku, Kyoto 606-8501, Japan*

Received 21 April 1998; revised 30 June 1998; accepted 30 June 1998

Abstract

Types of mutations induced by acrolein in the *supF* gene on the shuttle vector plasmid pMY189 replicated in normal human fibroblast cells were examined. Base sequence analysis of 92 plasmids with mutations in the *supF* gene revealed that the majority of the mutations were base substitutions (76%) and the others were deletions and insertions (24%). Single base substitutions were most frequently found (46%), while multiple base substitutions were 18% and tandem (two adjacent) base substitutions were 12% of the mutations. Of the base substitution mutations, G:C to T:A transversions were 44% and G:C to A:T transitions were 24%. The mutations were distributed not randomly but located at several hotspots. Acrolein produced DNA intra-strand cross-links between guanine residues, which might be responsible for rather high induction of the tandem base substitution mutations. © 1998 Elsevier Science B.V. All rights reserved.

Keywords: Acrolein; Mutation spectrum; *supF*; DNA intra-strand cross-link

1. Introduction

Acrolein (Fig. 1) is one of the α,β-unsaturated carbonyl compounds which are present in our environment as commonly-used industrial chemicals, natural products, environmental contaminants and products of the endogenous metabolism in human beings [1]. Acrolein is mutagenic to bacteria *Salmonella typhimurium* [2] and to human cells cultured from xeroderma pigmentosum (XP) patients [3] without metabolic activation.

Reaction of acrolein with deoxyguanosine has been shown to result in formation of 6-hydroxy $1,N^2$-propanodeoxyguanosine and 8-hydroxy $1,N^2$-propanodeoxyguanosine adducts (Fig. 1) in vitro [4]. These *a*crolein-derived hydroxypropano*d*eoxy*g*uanosines (AdGs) are detected in DNA of cultured

---

Abbreviations: XP: Xeroderma pigmentosum; AdGs: Acrolein-derived hydroxy $1,N^2$-propanodeoxyguanosines; PdG: $1,N^2$-Propanodeoxyguanosine; IPTG: Isopropyl-β-D-thiogalactoside; X-gal: 5-Bromo-4-chloro-3-indoyl-β-D-galactoside; PBS: Phosphate buffered saline; PCR: Polymerase chain reaction; cis-Pt: *cis*-Diamminedichloroplatinum(II); PAGE: Polyacrylamide gel electrophoresis

* Corresponding author. Tel.: +81-75-753-4412; Fax: +81-75-753-4419; E-mail: c51845@sakura.kudpc.kyoto-u.ac.jp

1383-5718/98/$19.00 © 1998 Elsevier Science B.V. All rights reserved.
PII: S1383-5718(98)00093-X

Table 1
Types of sequence alternations in *supF* gene in plasmids pMY189 replicated in normal human fibroblasts WI38-VA13

Types	No. of plasmids with mutations (%)	
	Acrolein-induced	Spontaneous
Base substitutions	70 (76)	25 (81)
Single	42 (46)	17 (55)
Tandem	11 (12)	1 (3)
Multiple	17 (18)[a]	7 (23)[d]
Deletions and insertions	22 (24)	6 (19)
Single base deletion	4 (4)[b]	0 (0)
≥ 2 bases deletion	16 (17)[c]	6 (19)
Single base insertion	0 (0)	0 (0)
≥ 2 bases insertion	2 (2)[c]	0 (0)
Total plasmids sequenced	92 (100)	31 (100)

Plasmids having base substitutions and deletions or insertions are listed in 'Deletions and insertions'.
[a]Two had accompanying tandem base substitutions.
[b]Three had other base substitutions.
[c]One had another base substitution.
[d]One had an accompanying tandem base substitution.

by G:C to C:G and A:T to T:A transversions (12% each). In the spontaneous mutants, almost all (33 of 34) base substitutions occurred at guanine or cytosine. Among them, G:C to T:A transversions were predominant (56%), followed by G:C to A:T transitions and G:C to C:G transversions (21% each).

Types of both acrolein-induced and spontaneous mutations were similar. However, the acrolein-induced mutations scarcely contain spontaneously occurring mutations because the mutants of which mutation frequency was at least 20 times higher than the spontaneous mutation frequency were used for sequence analysis.

3.3. Mutation spectrum

Distribution of the acrolein-induced base substitutions over the coding region of the *supF* tRNA gene is shown in Fig. 5A. Mutations were not distributed randomly ($P < 0.0005$) but were located mostly at specific sites. There were three hotspots (> 4 base changes), at sites 133, 159 and 160, where the number of mutations observed was 4-fold or more greater than the number expected for random distribution. The most prominent hotspot was at base pair 160, where almost all base substitutions (7 of 9) were transversions. All hotspots were located at the sites of G:C base pairs.

There were 13 tandem base substitutions; five were GG to AT (or CC to AT), four were GG to TT (CC to AA). Others were one each of GA to TT (TC to AA), GC to AT, AT to TG (AT to CA) and GT to TA (AC to TA). Most of the tandem base substitutions (9 of 13) occurred at GG (or CC) sites.

Distribution of the spontaneous base substitutions is shown in Fig. 5B. Mutations were located mostly at specific sites ($P < 0.0005$). The hotspot at site 133 in the *supF* gene was observed in both acrolein-induced and spontaneous mutants. Despite of some similarities between acrolein-induced and spontaneous hotspots, the induced mutations should be ascribed to DNA damage by acrolein, because mutation frequency of the acrolein-induced mutations used for the analysis was at least 20-fold higher than the spontaneous mutation frequency.

3.4. Detection of intra-strand crosslinks

Approximately one-tenth of the mutated plasmids had tandem base substitutions (Table 1), mainly at GG (or CC) sites (Fig. 5), suggesting that they might be arisen from intra-strand crosslinks. As the UV-induced pyrimidine dimers [20,21] or *cis*-Pt-induced intra-strand cross-links [22] are shown to yield tandem base substitutions, we assumed that acrolein induced intra-strand crosslinks in DNA.

Fig. 6 shows that the 40 mer products, presumably formed by the GG intra-strand cross-links, were detected on the lane where the acrolein-treated 20 mer substrates were loaded. The possibility that the

Table 2
Types of base substitutions is *supF* gene in plasmids replicated in normal human fibroblasts WI38-VA13

Base substitutions	No. of base changes (%)	
	Acrolein-induced	Spontaneous
G:C to T:A	48 (44)	19 (56)
G:C to A:T	26 (24)	7 (21)
G:C to C:G	13 (12)	7 (21)
A:T to T:A	13 (12)	0 (0)
A:T to C:G	5 (5)	1 (0.3)
A:T to G:C	4 (4)	0 (0)
Total	108 (100)	34 (100)

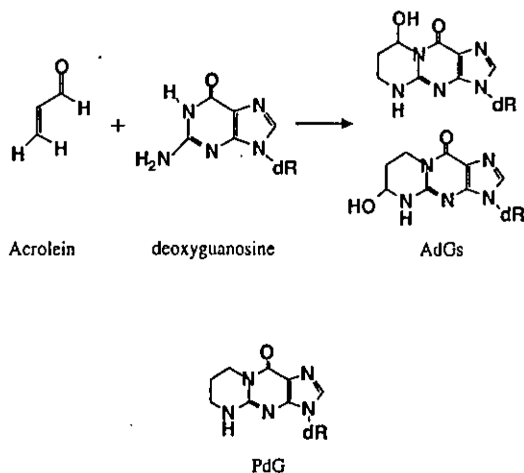

Fig. 1. Acrolein, two forms of acrolein-derived hydroxy 1, N^2-propanodeoxyguanosine (AdGs) and propanodeoxyguanosine (PdG).

human fibroblast cells treated with acrolein and in peripheral blood lymphocytes obtained from a dog given cyclophosphamide [5]. AdGs are present in DNA of various human and rodent tissues without any carcinogen treatment [6] as well as in DNA of culture Chinese hamster ovary cells treated with acrolein [7,8]. Metabolic conversion yielding AdGs was suggested in these studies.

Site-directed mutagenesis studies with viral or plasmid DNA using 1,N^2-propanodeoxyguanosine (PdG) (Fig. 1), which is structurally similar to AdGs, demonstrate that the PdG causes frameshifts (deletions) and base substitutions in the DNA propagated in bacteria and mammalian cells. When viral DNA containing PdG in the CG repeats is introduced into *Escherichia coli*, frameshift mutations are frequently detected [9]. When plasmids containing the PdG are replicated in simian kidney (COS) cells or in *E. coli*, the predominant base substitution is PdG to T in both cells, and a significantly high frequency of PdG to A substitution in the plasmids is also reported in *E. coli* [10–12].

Although the mutational specificity of PdG is well known, the spectrum of mutations by acrolein is still unknown. We produced DNA damage in shuttle vector plasmids pMY189 by acrolein treatment, and frequencies and types of mutations in the *supF* gene of the plasmids propagated in human cells were investigated.

2. Materials and methods

2.1. Chemicals

Acrolein (purity > 99.9%, CAS 107-02-8), ampicillin, chloramphenicol, nalidixic acid, isopropyl-β-D-thiogalactoside (IPTG) and 5-bromo-4-chloro-3-indoyl-β-D-galactoside (X-gal) were obtained from Wako (Osaka, Japan). Restriction endonuclease *Dpn*I was purchased from New England Biolabs, (Beverly, MA). Qiagen plasmid-kit, QIAprep-spin Plasmid kit and QIAquick-spin PCR Purification kit were obtained from Qiagen (Hilden, Germany). Three kinds of 20 mer single-strand DNA (i.e., 5′-TCGTGACTGGGAAAACCCTG-3′, 5′-GCGTTACCCAACTTAATCGC-3′, 5′-CTTGCAGCACATCCCCCTTT-3′) and 5′-Biotinated 20 mer single-strand DNA (i.e., 5′-TTAACGCGAATTTTAACAAA-3′) were synthesized by Nippon Seihun (Tokyo, Japan). pBluescript KS(−) was purchased from Toyobo (Tokyo, Japan). *Taq* polymerase was obtained from Takara Shuzo (Kyoto, Japan). Dynabeads M-280 streptavidin was obtained from Dynal (Oslo, Norway). [γ-^{32}P] ATP was purchased from Amersham (Chiba, Japan).

2.2. Cells

An SV40-transformed normal human fibroblast cell line WI38-VA13 [13] was obtained from the American Type Culture Collection (Rockville, MD). DNA repair deficient XP20S(SV) cells were established by us from a Japanese group A XP patient [14]. All cells were cultured in Dulbecco's modified minimum essential medium (Nikken, Kyoto, Japan) supplemented with 10% fetal bovine serum (Hyclone, Logan, UT).

2.3. Shuttle vector plasmid and bacterial strains

The shuttle vector plasmid pMY189, constructed by Matsuda et al. [15], was used for analysis of mutations. The pMY189 was derived from the pZ189 [16] as described previously [15]. The indicator *E. coli* strain KS40/pKY241 [17] is a nalidixic acid-resistant (*gyrA*) derivative of MBM7070 (*lacZ* (am) *CA7070 lacYl HsdR HsdM* Δ (*araABC-leu*)*7679*

galU galK rpsL thi) [18], which has been used for detection of the mutated pZ189. The plasmid pKY241 was constructed by Akasaka et al. [17] and contains a chloramphenicol resistant marker and a *gyrA* (amber) gene. *E. coli* KS40/pKY241 cells carrying the active *supF* gene are sensitive to nalidixic acid, whereas the cells carrying the mutated *supF* form colonies on the selection plates containing nalidixic acid, chloramphenicol and ampicillin. *E. coli* cells containing the active *supF* gene produce blue colonies, whereas cells having the mutated *supF* gene produce white or light blue colonies on the selection plates.

2.4. Treatment of plasmids with acrolein, transfection to human cells, and plasmid recovery

Purified stocks of pMY189 were prepared by using the QIAGEN plasmid purification kit. The plasmids (30 μg) were treated with various concentrations of acrolein in total volume of 0.5 ml of 0.1M sodium phosphate buffer (pH 7.4). The reaction was allowed to proceed for 15 h at 37°C followed by ethanol precipitation of the plasmids to remove the non-reacted excess acrolein, and the plasmids were redissolved in 400μl of Dulbecco's phosphate buffered saline (PBS) solution (pH 7.5).

The human cells (2×10^7), WI38-VA13 or XP2OS(SV), and 15 μg acrolein-treated pMY189 in PBS solution (200 μl) were placed in an electroporation chamber (electrodes 0.3 cm apart) (PDS, Madison, WI) and the cells were transfected with the plasmids by electric pulses (600 V, 4 times). The cells were plated in 10-cm dishes and incubated at 37°C for 72 h in a CO_2 incubator. Then plasmids were extracted from the cells using the QIAprep-spin Plasmid kit. The purified plasmids were digested with the restriction endonuclease *Dpn*I to eliminate non-replicated plasmids which retain the bacterial methylation pattern.

2.5. Selection of mutated supF, and determination of DNA base sequences

Plasmid DNA replicated in the human cells was introduced into the indicator bacteria KS40/pKY241 by the electroporation apparatus *E. coli* Pulsar (Bio-Rad Laboratories, Hercules, CA). The bacteria cells were plated on LB agar containing 50 μg/ml nalidixic acid, 150 μg/ml ampicillin and 30 μg/ml chloramphenicol, IPTG and X-gal to select the plasmids containing the mutated *supF* genes. A portion of the cells was plated on LB agar containing ampicillin and chloramphenicol to measure the total number of transformants. After the plates were incubated for 24 h at 37°C, colonies were counted and mutation frequencies were calculated.

E. coli having mutated plasmids which had been propagated in normal cells were cultured overnight. Then the plasmids were extracted and purified with the QIAprep-spin Plasmid kit and the size of the mutated plasmid was checked by agarose gel electrophoresis. The base sequences of the *supF* gene of the plasmids which were not aberrant in size were determined with the ABI PRISM™ Dye Primer (-21M13) Cycle Sequencing Ready Reaction Kit (Perkin-Elmer, Foster, CA) using the 370A automatic DNA sequencer (Perkin-Elmer, Foster, CA). The mutants having the identical base changes derived from the same transfection plate were not scored to exclude clusters of the same clones.

The χ^2-goodness of fit test was used to determine if the acrolein-induced base substitution mutations were distributed randomly or non-randomly over the coding region of the *supF* tRNA gene [19].

2.6. Detection of intra-strand cross-links

A part of pBluescript KS(−) sequences (175 base pairs) was amplified with TaKaRa Ex *Taq* polymerase (total reaction volume was 50μl) by the polymerase chain reaction (PCR) using following two primers: 5′-TCGTGACTGGGAAAACCCTG-3′ and 5′-Biotinated-TTAACGCGAATTTTAACAAA-3′. The PCR conditions were composed of 30 cycles of 94°C for 0.5 min, 55°C for 0.5 min and 72°C for 1 min. The PCR products were purified with the QIAquick-spin PCR Purification kit. About 14 pmol of the PCR products were obtained. These biotinated 175 mer double stranded-DNA were immobilized to Dynabeads M-280 streptavidin. After the 175 mer DNA was denatured with 0.1 M NaOH and washed with 0.1 M NaOH and TE buffer containing 1M NaCl on a magnet, single stranded 175 mer DNA immobilized to Dynabeads M-280 streptavidin were

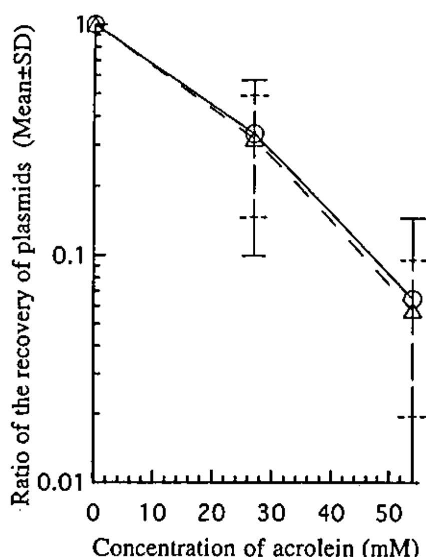

Fig. 2. Survival of the acrolein-treated pMY 189 plasmids propagated in repair-proficient WI38-VA13 (O) and repair-deficient XP2OS(SV) (△) cells. The ratio of the number of ampicillin-resistant bacterial colonies with acrolein-treated plasmids to those with the untreated plasmids is shown. Average numbers of three independent experiments are plotted with the S.D.

obtained. The immobilized DNA sequences are as follows: 5′-immobilized-TTAACGCGAATTTT-AACAAAATATTAACGCTTACAATTTCCATTC-GCCATTCAGGCTGCGCAACTGTTGGGAAGG-GCGATCGGTGCGGGCCTCTTCGCTATTACGC-CAGCTGGCGAAAGGGGGATGTGCTGCAAGG-CGATTAAGTTGGGTAACGCCAGG GTTTTC-CCAGTCACGA-3′ Two kinds of DNA (i.e., 5′-TCGTGACTGGGAAAACCCTG-3′ and 5′-GCGTTACCCAACTTAATCGC-3′) were labeled with ^{32}P by treatment with bacteriophage T4 polynucleotide kinase and [γ-^{32}P] ATP. The immobilized single-stranded 175 mer DNA was annealed with ^{32}P labeled 5′-TCGTGACTGGGAAAACCCTG-3′ and non-labeled 5′-GCGTTACCCAACTTAATCGC-3′, or with ^{32}P labeled 5′-GCGTTACCCAACTTAATCGC-3′ and non-labeled 5′-CTTGCAGCACATCCCCCTTT-3′, by heating and cooling in 1 M NaCl for detecting a GG-intrastrand crosslink or a CC-intrastrand crosslink, respectively (Fig. 2, '1 Preparation of substrates').

The annealed DNA (1 pmol of each) was treated with 54 mM of acrolein in 0.05 M sodium phosphate buffer (pH7.4) containing 0.1 M NaCl for 24 h at 4°C (Fig. 2, '2 Treatment of substrates with acrolein'). DNA was collected by a magnet and redissolved in 10μl of 0.1M NaCl. Then DNA solution was mixed with 2 μl of dye (50% urea, 15% glycerol, 0.25% bromophenolblue, 0.25% xylenecyanol), and separated by 12% polyacrylamide gel (50% urea, 1 × TBE) electrophoresis for 45 min at 500 V. The gel was exposed to X-ray films for autoradiography (Fig. 2, '3 PAGE and Autoradiography').

3. Results

3.1. Recovery and mutation of plasmids

The acrolein-treated plasmids were inactivated with an increase in concentration of acrolein. They were not apparently subjected to the nucleotide excision repair because no difference in the plasmid recovery was found when they were propagated in normal and XP cells (Fig. 3). Lack of the repair was

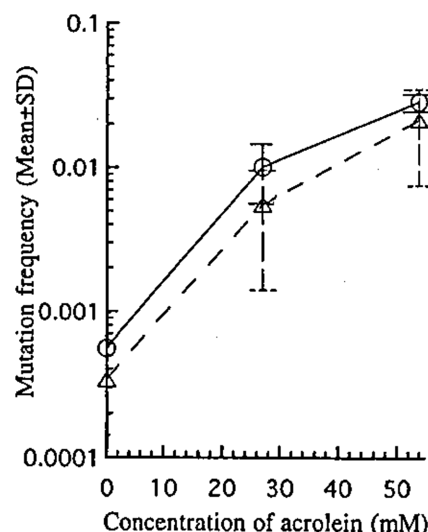

Fig. 3. Mutation frequency of the acrolein-treated pMY 189 plasmids propagated in repair-proficient WI38-VA13 (O) and repair-deficient XP2OS(SV) (△) cells. Average numbers of three independent experiments are plotted with the S.D.

A: Acrolein-induced

```
100       110       120       130       140       150       160       170       180
 +         +         +         +         +         +         +         +         +
GGTGGGGTTCCCGAGCGGCCAAAGGGAGCAGACTCTAAATCTGCCGTCATCGACTTCGAAGGTTCGAATCCTTCCCCCACCACCA
TTGT   G GA AGTG T  TC TT TAT C   GA  G AG   TAT  A T   AA  TT  TTTT AT  G  AT  T AA
TT           TT         TTT A     GA    A    C           A  AT       AT  T  AA
AT           TC         T   A     GA    A                   AT       AA      T
                        A   T     GC    A                   AT       A
                                  G                         TT
                                  A                          T
                                  A                          T
                                  A                          A
                                                             A
                                                             C
```

B: Spontaneous

```
100       110       120       130       140       150       160       170       180
 +         +         +         +         +         +         +         +         +
GGTGGGGTTCCCGAGCGGCCAAAGGGAGCAGACTCTAAATCTGCCGTCATCGACTTCGAAGGTTCGAATCCTTCCCCCACCACCA
         TTG            T         G     A      A  T  AC A       TC   A
         T                        G     A               A       TC   A
         T                        G     A               A        T   A
                                  A                     G            A
                                                        T            T
```

Fig. 4. Distribution of the base substitutions in *supF* tRNA gene in plasmids pMY189 replicated in normal human fibroblasts WI38-VA13. Acrolein-induced (A) and spontaneous (B) mutations are shown. Underlined bases are with tandem base substitutions. Sites corresponding to tRNA coding sequences (99–183) are shown. Multiple mutations, deletions and insertions are as follows (the site of the change is shown in parenthesis); Acrolein-induced: G to T (32) + C to A (168); G to A (43) + T to A (45); A to T (66) + T to G (67) + G to T (160); C to T (80) + C to A (109) + C to T (110); T to G (101) + A to C (120); T to G (106) + C to A (149); A to T (112) + C to T (179); G to T (113) + G to T (116); A to T (125) + C to T (127); C to G (133) + C to T (146); C to G (133) + C to A (182); C to A (139) + C to A (181); A to T (151) + C to T (172); G to A (159) + C to T (163) + A to G (165); G to T (164) + A to T (166); C to A (168) + C to T (185); C to G (172) + C to A (176); 41 base pairs insertion (6–16) + G to C (129); deletion (16–121); deletion (19–122); deletion (30–197); C to T (30) + deletion (99) + G to T (102); deletion (42–139); deletion (82–183); deletion (94–132); deletion (95–127); deletion (96–133); deletion (99) + G to T (102); deletion (107–117); deletion (110–111) + C to G (114) + A to T (119); G to A (111) + deletion (114); deletion (115–212); deletion (125–228); 31 base pairs insertion (136–137); deletion (144); deletion (152–187); deletion (167–202); TTCCCC to AA (170–175); *supF* sequence ended at 90 bp; Spontaneous: G to T (65); C to T (108) + C to T (155); C to G (110) + C to G (155); C to G (133) + C to A (146) + C to A (168); C to T (149) + C to T (163) + C to A (185); C to A (155) + C to T (220); C to T (163) + C to A (185); deletion (45–128); deletion (117–129); deletion (117–387); deletion (128–165); deletion (133–157); deletion (144–219).

also demonstrated in the acrolein-induced mutations because no difference in mutation frequencies was detected after the acrolein-treated plasmids were propagated in normal and XP cells (Fig. 4).

3.2. Base sequence analysis

Types of mutations in *supF* gene of the plasmids replicated in normal cells were examined (Table 1). The majority (76%) of acrolein-induced mutations were base substitutions. About half of the mutant plasmids had a single base substitution, while 12% and 18% of them had tandem (adjacent two base substitutions) and multiple (≥ 2 base substitutions except for the tandem base substitutions) mutations, respectively. Twenty two (24%) plasmids had deletions or insertions and five of them had base substitutions as well. The majority (81%) of spontaneous mutations were also base substitutions. Seventeen (55%) spontaneous mutant plasmids had a single base substitution and seven (23%) of them had multiple base substitutions. Six (19%) plasmids had deletions.

Types of the base substitutions are shown in Table 2. The majority of the acrolein-induced base substitutions (80%) occurred at guanine or cytosine. The most frequent mutations were G:C to T:A transversions (44%), and the other frequent mutations were G:C to A:T transitions (24%), followed

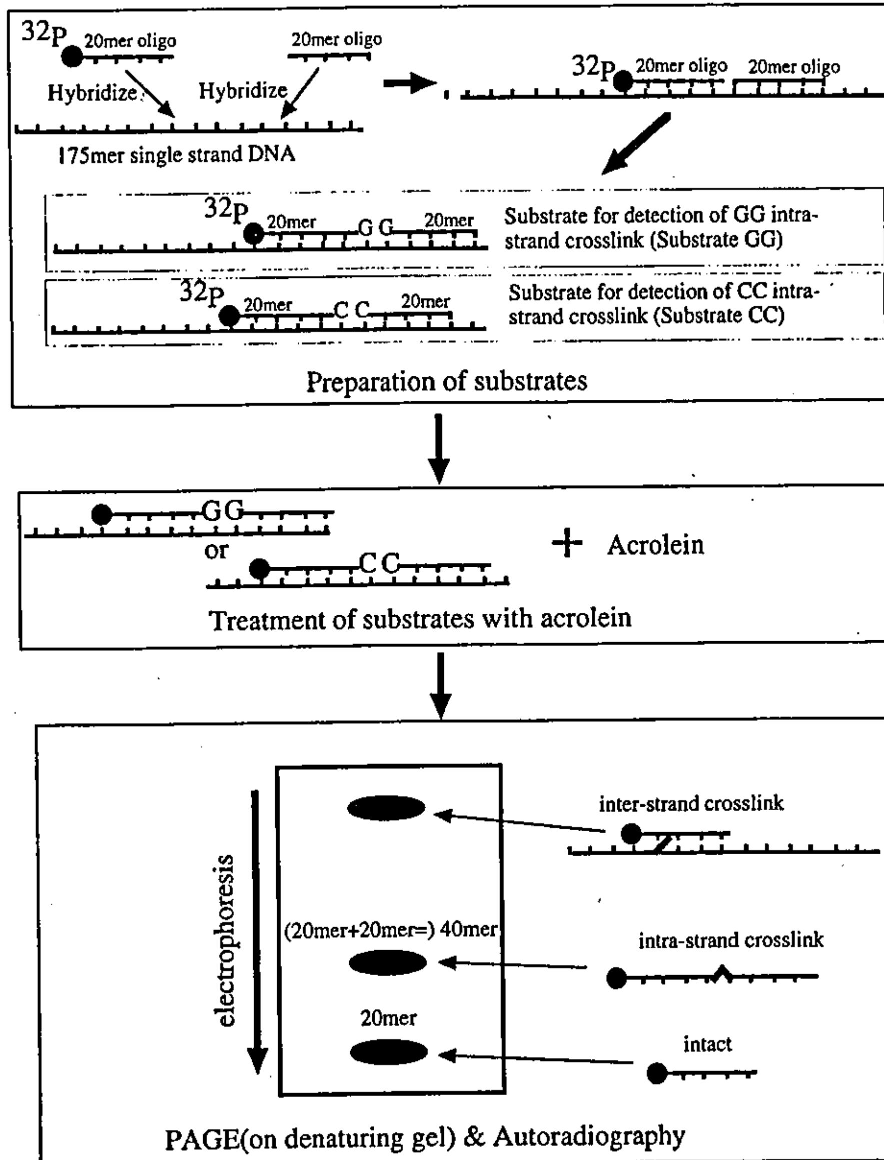

Fig. 5. Experimental procedure for detection of the intra-strand cross-links. (1) Preparation of substrates: A single-stranded 175 mer DNA was annealed with a ^{32}P-labeled 20 mer oligo nucleotide and a non-labeled 20 mer oligo nucleotide for an intra-strand cross-link detection. Two kinds of substrates were prepared. One is for a GG intra-strand cross-link detection and the other is for a CC intra-strand cross-link detection. (2) Treatment of substrates with acrolein: the annealed DNA was treated with acrolein. (3) PAGE and Autoradiography: DNA was separated by polyacrylamide gel (50% urea) electrophoresis. The gel was exposed to X-ray films for autoradiography.

40 mer products formed by reacting ^{32}P-20 mer nucleotides with unlabeled 20 mer or ^{32}P-20 mer nucleotides without 175 mer single strand DNA is ruled out because ^{32}P-20 mer nucleotides which were not annealed with 175 mer DNA were undetectable in the reaction mixture (data not shown). No 40 mer products appeared on the lane in which CC intra-strand crosslinks might have formed. These results indicate that acrolein forms a molecular bridge between adjacent guanine bases in the same strand of

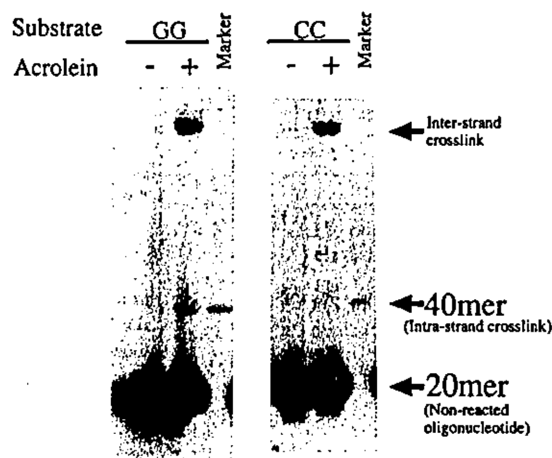

Fig. 6. Detection of DNA intra-strand crosslinks formed by acrolein. GG and CC show substrates for detection of GG and CC intra-strand crosslinks (see Fig. 5), respectively. Marker: 40 mer single-strand DNA.

DNA. The bands corresponding to the acrolein-induced inter-strand crosslinks appeared on both lanes. However, the biological consequences of the inter-strand cross-links have not been studied.

4. Discussion

Majority (80%) of the acrolein-induced base substitutions took place at guanine or cytosine residues. These results are consistent with previous studies using PdG which has a structure similar to AdGs. The propano adducts cause G to T transversions in both mammalian and *E. coli* cells, and also G to A transitions in *E. coli* [10–12]. As shown in Table 2, the most frequently identified base substitutions were G:C to T:A transversions and the other frequent mutations were G:C to A:T transitions. Such mutation specificity of acrolein is similar to that of PdG, possibly due to the structural similarity between PdG and AdGs.

Twenty-two base substitutions (22%) were found at A:T sites. Marnett et al. [2] reported that acrolein induces base pair substitution mutations without the metabolic activation in *Salmonella* TA104 in which the mutational site is the nonsense sequences TAA. Acrolein produces a little amount of 1,N^6-propanodeoxyadenosine as well as guanosine adducts [23]. This propanodeoxyadenosine adduct may lead to the mutation at A:T sites.

Thirteen of the 92 mutant plasmids (14%) contained tandem base substitutions and most of these tandem base substitutions (9 of 13) occurred at GG (or CC) sites. There has been no previous report that the acrolein or propano adduct induces tandem base substitutions. It has been shown that tandem base substitutions are produced by UV [20,21] and *cis*-diamminedichloroplatinum(II) (*cis*-Pt) [22]. UV induces pyrimidine dimers, and *cis*-Pt causes intra-strand crosslinks in DNA. We showed that acrolein forms a molecular bridge between adjacent guanine bases in the same strand of DNA. This intra-strand cross-link might be a cause of the tandem base substitutions which were found in the acrolein-treated *supF* gene. The molecular structure of this cross-link is not elucidated. Acrolein is a bifunctional compound and therefore it could form a molecular bridge in DNA.

Curren et al. [3] reported that acrolein was strongly mutagenic to the nucleotide excision-repair deficient XP fibroblast cells, while it did not induce mutations in normal fibroblasts. Recent studies have shown that PdG could be repaired by the nucleotide excision repair system [24]. As the structural difference between PdG and AdGs is presence or absence of a hydroxy group (Fig. 1), it is unlikely that PdG and AdGs are repaired by different pathways. In our study, however, acrolein-treated plasmids pMY189 yielded the same frequency of mutations in XP cells and normal cells (Fig. 4). The possibility that DNA repair capability of the host cells does not affect the repair of the shuttle vector plasmids is ruled out because UV-irradiated *supF* shuttle vector plasmids showed higher mutation frequencies in XP2OS (SV) cells than in WI38-VA13 cells [21]. Our results suggest that the major repair pathway of acrolein-induced DNA damage in human cells is not the nucleotide excision repair system.

Acknowledgements

This work was supported by the Grant-in-Aid from Ministry of Education, Science, Sports and Culture of Japan and a fellowship (to M.K.) by Japan Society for the Promotion of Science.

References

[1] L.J. Marnett, DNA Adducts of α,β-unsaturated aldehydes and dicarbonyl compounds, in: DNA adducts Identification and Biological Significance, International Agency for Research on Cancer, Lyon, 1994, pp. 151–163.

[2] L.J. Marnett, H.K. Hurd, M.C. Hollstein, D.E. Levin, H. Esterbauer, B.N. Ames, Naturally occurring carbonyl compounds are mutagens in *Salmonella* tester strain TA104, Mutat. Res. 148 (1985) 25–34.

[3] R.D. Curren, L.L. Yang, P.M. Conklin, R.C. Grafstrom, C.C. Harris, Mutagenesis of xeroderma pigmentosum fibroblasts by acrolein, Mutat. Res. 209 (1988) 17–22.

[4] F.L. Chung, R. Young, S.S. Hecht, Formation of cyclic $1,N^2$-propanodeoxyguanosine adducts in DNA upon reaction with acrolein or crotonaldehyde, Cancer Res. 44 (1984) 990–995.

[5] V.L. Wilson, P.G. Foiles, F.L. Chung, A.C. Povey, A.A. Frank, C.C. Harris, Detection of acrolein and crotonaldehyde DNA adducts in cultured human cells and canine peripheral blood lymphocytes by ^{32}P-postlabeling and nucleotide chromatography, Carcinogenesis 12 (1991) 1483–1490.

[6] R.G. Nath, F.L. Chung, Detection of exocyclic $1,N^2$-propanodeoxyguanosine adducts as common DNA lesions in rodents and humans, Proc. Natl. Acad. Sci. U.S.A. 91 (1994) 7491–7495.

[7] R.G. Nath, J.E. Ocando, F.L. Chung, Detection of $1,N^2$-propanodeoxyguanosine adducts as potential endogenous DNA lesions in rodent and human tissues, Cancer Res. 56 (1996) 452–456.

[8] P.G. Foiles, S.A. Akerkar, L.M. Miglietta, F.L. Chung, Formation of cyclic deoxyguanosine adducts in Chinese hamster ovary cells by acrolein and crotonaldehyde, Carcinogenesis 11 (1990) 2059–2061.

[9] M. Benamira, U. Singh, L.J. Marnett, Site-specific frameshift mutagenesis by a propanodeoxyguanosine adduct positioned in the $(CpG)_4$ hot-spot of *Salmonella typhimurium* hisD3052 carried on an M13 vector, J. Biol. Chem. 267 (1992) 22392–22400.

[10] M. Moriya, W. Zhang, F. Johnson, A.P. Grollman, Mutagenic potency of exocyclic DNA adducts: marked differences between *Escherichia coli* and simian kidney cells, Proc. Natl. Acad. Sci. U.S.A. 91 (1994) 11899–11903.

[11] P.C. Burcham, L.J. Marnett, Site-specific mutagenesis by a propanodeoxyguanosine adduct carried on an M13 genome, J. Biol. Chem. 269 (1994) 28844–28850.

[12] S.P. Fink, G.R. Reddy, L.J. Marnett, Relative contribution of cytosine deamination and error-prone replication to the induction of propanodeoxyguanosine → deoxyadenosine mutations in *Escherichia coli*, Chem. Res. Toxicol. 9 (1996) 277–283.

[13] A.J. Girardi, F.C. Jensen, H. Koprowski, SV40-induced transformation of human diploid cells, crisis and recovery, J. Cell. Comp. Physiol. 62 (1965) 69–84.

[14] H. Takebe, S. Nii, M.I. Ishii, H. Utsumi, Comparative studies of host-cell reactivation, colony forming ability and excision repair after UV irradiation of xeroderma pigmentosum, normal human and some other mammalian cells, Mutat. Res. 25 (1974) 383–390.

[15] T. Matsuda, T. Yagi, M. Kawanishi, S. Matsui, H. Takebe, Molecular analysis of mutations induced by 2-chloroacetaldehyde, the ultimate carcinogenic form of vinyl chloride, in human cells using shuttle vectors, Carcinogenesis 16 (1995) 2389–2394.

[16] K.H. Kraemer, M.M. Seidman, Use of *supF*, an *Escherichia coli* tyrosine suppressor tRNA gene, as a mutagenic target in shuttle-vector plasmids, Mutat. Res. 220 (1989) 61–72.

[17] S. Akasaka, K. Takimoto, K. Yamamoto, G,C → T,A and G,C → C,G transversions are the predominant spontaneous mutations in the *Escherichia coli supF* gene; an improved *lacZ(am) E. coli* host designed for assaying pZ189 *supF* mutational specificity, Mol. Gen. Genet. 235 (1992) 173–178.

[18] M.M. Seidman, K. Dixon, A. Razzaque, R. Zagursky, M.L. Berman, A shuttle vector plasmid for studying carcinogen-induced point mutations in mammalian cells, Gene 38 (1985) 233–237.

[19] G.W. Snedecor, W.G. Cochran, Statistical Methods, Iowa State Univ. Press, Ames, 1967.

[20] E.A. Drobetsky, A.J. Grosovsky, B.W. Glickman, The specificity of UV-induced mutations at an endogenous locus in mammalian cells, Proc. Natl. Acad. Sci. U.S.A. 84 (1987) 9103–9107.

[21] T. Yagi, J. Tatsumi-Miyajima, M. Sato, K.H. Kraemer, H. Takebe, Analysis of point mutations in an ultraviolet-irradiated shuttle vector plasmid propagated in cells from Japanese xeroderma pigmentosum patients in complementation groups A and F, Cancer Res. 51 (1991) 3177–3182.

[22] G.J. Bubley, B.P. Ashburner, B.A. Teicher, Spectrum of cis-diamminedichloroplatinum(II)-induced mutations in a shuttle vector propagated in human cells, Mol. Carcinog. 4 (1991) 397–406.

[23] R.A. Smith, D.S. Williamson, R.L. Cerny, S.M. Cohen, Detection of $1,N^6$-propanodeoxyadenosine in acrolein-modified polydeoxyadenylic acid and DNA by ^{32}P postlabeling, Cancer Res. 50 (1990) 3005–3012.

[24] K.A. Johnson, S.P. Fink, L.J. Marnett, Repair of propanodeoxyguanosine by nucleotide excision repair in vivo and in vitro, J. Biol. Chem. 272 (1997) 11434–11438.

Environ. Sci. Technol. 2004, *38*, 6424–6429

Detection of Genistein as an Estrogenic Contaminant of River Water in Osaka

MASANOBU KAWANISHI,[†]
TAKEJI TAKAMURA-ENYA,[‡]
RAHYANI ERMAWATI,[§]
CHIAKI SHIMOHARA,[†]
MICHIYO SAKAMOTO,[†]
KAZUKI MATSUKAWA,[†]
TOMONARI MATSUDA,[§]
TSUYOSHI MURAHASHI,[||]
SABURO MATSUI,[§] KEIJI WAKABAYASHI,[‡]
TETSUSHI WATANABE,[||]
YUTAKA TASHIRO,[⊥] AND
TAKASHI YAGI[*,†]

Research Institute for Advanced Science and Technology, Osaka Prefecture University, 1-2 Gakuen-cho Sakai, Osaka 599-8570, Japan, Cancer Prevention Basic Research Project, National Cancer Center Research Institute, 1-1 Tsukiji 5-Chome, Chuo-ku, Tokyo 104-0045, Japan, Department of Environmental Engineering, Kyoto University Graduate School, Sakyo-ku Yoshida-Honmachi, Kyoto 606-8501, Japan. Department of Public Health, Kyoto Pharmaceutical University, 5 Misasagi Nakauchicho, Yamashina-ku, Kyoto 607-8414, Japan, and Okinawa Environmental Analysis Center Co. Ltd., 3-11-7 Maehara, Ginowan, Okinawa 901-2215, Japan

The estrogenic activity in water at various localities on Lake Biwa–Yodo River, a representative watershed in Japan, was measured using a recombinant yeast that expresses the human estrogen receptor. The yeast bioassay revealed that the activities of 13 water samples had an average value of 14 pmol/L (3.8 ng/L) (17β-estradiol equivalent) with a very wide range from 0 to 72 pmol/L (0–19.6 ng/L), and two of the samples had prominent levels of activity (72 pmol/L (19.6 ng/L) and 56 pmol/L (15.2 ng/L)). We analyzed these two samples with instrumental approaches. A high-performance liquid chromatogram profile showed that the strong activity in one sample, which was collected just downstream of a sewage-treatment plant, would be due to 17β-estradiol and estrone, whose source is considered to be human urine contained in the effluent of the plant. The activity in the other sample, which was obtained from a tributary river in a primarily residential area with some industrial development (i.e., Osaka City), however, did not correspond to 17β-estradiol, estrone, or synthetic chemicals known as estrogenic. Analysis of a fraction with estrogenic activity by liquid chromatography–mass spectrometry (LC–MS) provided evidence that the activity in the water sample resulted from the presence of genistein, an isoflavone compound of plant origin.

* Corresponding author phone: +81-72-254-9862; fax: +81-72-254-9938; e-mail: yagi-t@riast.osakafu-u.ac.jp.
† Osaka Prefecture University.
‡ National Cancer Center Research Institute.
§ Kyoto University Graduate School.
|| Kyoto Pharmaceutical University.
⊥ Okinawa Environmental Analysis Center Co. Ltd.

Introduction

Lake Biwa–Yodo River is a watershed located in the mid-western part of Japan. The catchment area of the watershed is 8240 km^2 and contains megalopolis Kyoto and Osaka where 12 million people live. This watershed has Lake Biwa in the upper part where the Uji River (Seta River) runs out as the main stream. The Uji River and two major tributaries, the Katsura and Kizu Rivers, join in the middle, and then the Yodo River runs as the main stream to Osaka Bay. The Kanzaki River branches out from the Yodo River in the lower reaches and also runs to Osaka Bay (Figure 1). In the upper basin of the watershed, land is used principally as cultivated fields, and the lower area is urbanized and industrialized. There are several reports on the genotoxicity of water in the Yodo River systems (*1–5*), and phenylbenzotriazole (PBTA)-type compounds are detected as major mutagens (*4–7*). Studies indicate that PBTA-type mutagens originate from azo dyes that are used as industrial materials for textile dyeing (*5–7*). Since this river system is the major source of drinking water for 16 million residents and the habitat of a large number of wildlife, the water quality should be monitored and maintained.

For decades, damage to the reproductive and developmental systems has been found in wild animals such as fish, waterfowl, and frogs. This is thought to be partly caused by environmental contaminants that inadvertently mimic the activities of vertebrate hormones (*8*). These contaminants, especially human estrogen-like substances, are called endocrine-disrupting substances. A very wide range of natural and man-made chemicals have now been found to be weakly estrogenic (*9–12*). For the last several years, the Japanese government has been investigating contamination by potential endocrine disrupters in the water environment (*13*). However instrumental analysis, which the governmental investigation has adopted, provides reliable data only when the analytes are known, and there are analytical standards available for quantitative analysis.

Several years ago, Routledge and Sumpter (*14*) developed a reporter gene assay with a recombinant strain of yeast that expresses the human estrogen receptor. In this yeast estrogenicity screening (YES) assay, the level of β-galactosidase activity indicates the level of ER signaling activated by ligand binding. Therefore, this bioassay system can be a powerful tool to evaluate total estrogenic activity in environmental samples. In this study, we measured the estrogenic activities of 13 water samples from Lake Biwa–Yodo River with the YES assay and adopted a toxicity identification evaluation (TIE) approach (*15*) to identify causal estrogenic compounds.

Experimental Section

Materials. Daidzein, genistin (genistein 7-*O*-β-D-glucopyranoside) and HPLC (high-performance liquid chromatograph)-grade acetonitrile were obtained from Sigma-Aldrich Japan Co. Ltd. (Tokyo, Japan). Bis(2-ethylhexyl) phthalate, estrone (E1), 17β-estradiol (E2), *p*-*n*-nonylphenol, and genistein were purchased from Wako Pure Chemical Industries (Osaka, Japan). All other chemicals used were of analytical grade and obtained from Sigma-Aldrich Japan Co. Ltd.

10.1021/es049764v CCC: $27.50 © 2004 American Chemical Society
Published on Web 08/18/2004

TABLE 1. Details of Sampling

point	location	date
1	Kunijima, Higashiyodogawa Ward, Osaka City, Osaka	Mar 28, 2002
2	Kitaeguchi, Higashiyodogawa Ward, Osaka City, Osaka	Mar 28, 2002; May 20, 2003
3	Hirakata Bridge, Hirakata City, Osaka	Mar 28, 2002
4	Kuzuha, Hirakata City, Osaka	Mar 28, 2002
5	Goko Bridge (Kizu River), Yawata City, Kyoto	Mar 28, 2002
6	Goko Bridge (Uji River), Yawata City, Kyoto	Mar 28, 2002
7	Koga Bridge, Minami Ward, Kyoto City, Kyoto	Mar 28, 2002
8	Kuze Bridge, Minami Ward, Kyoto City, Kyoto	Mar 28, 2002
9	Nango, Otsu Ctiy, Shiga	Mar 30, 2002
10	Yabase-Kihanto, Kusatsu City, Shiga	Mar 30, 2002
11	Ogoto, Otsu City, Shiga	Mar 30, 2002
12	Ishidera, Hikone City, Shiga	Mar 30, 2002
13	Funaki, Adogawa Town, Shiga	Mar 30, 2002

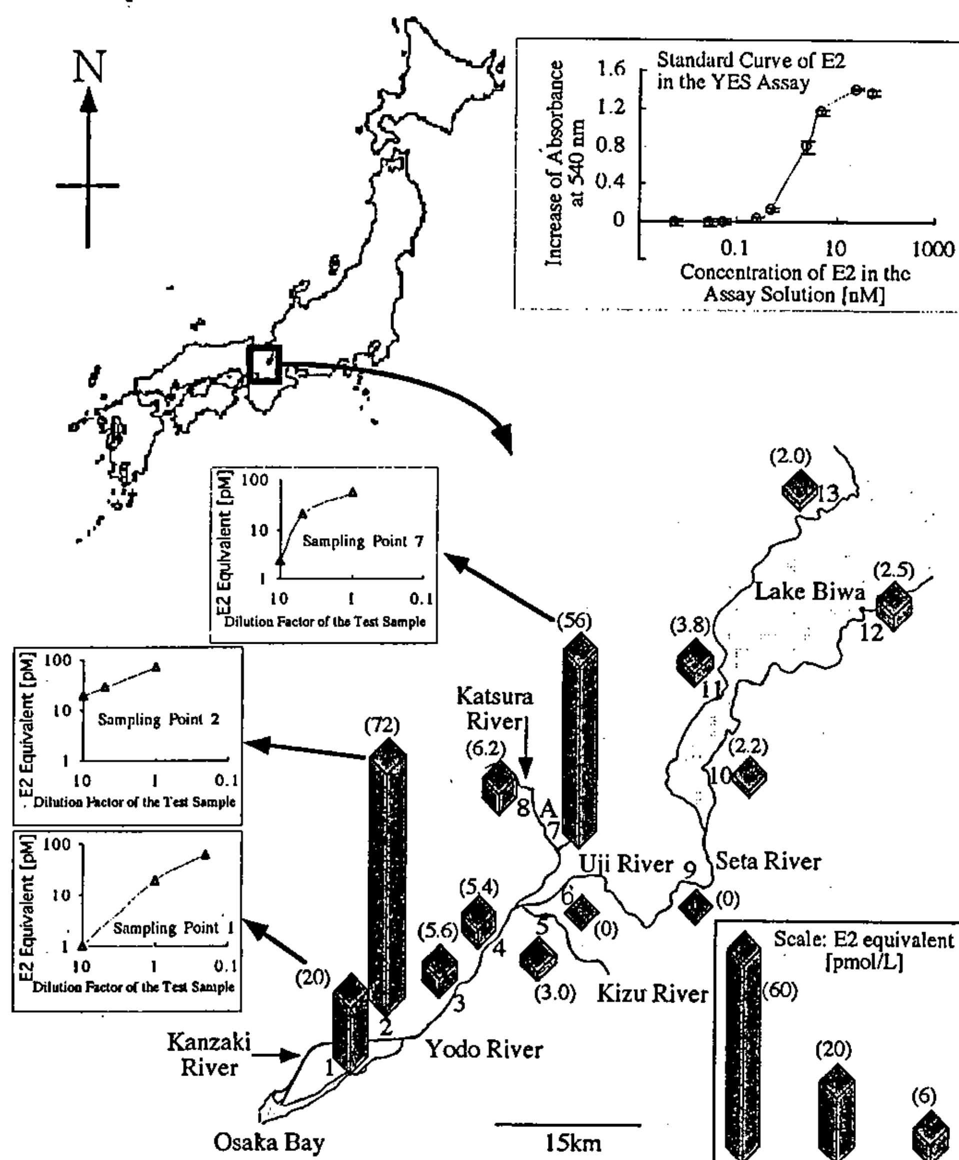

FIGURE 1. Location of the Lake Biwa–Yodo River system and estrogenic activity of original water samples at each point in March 2002. The sampling points are numbered from 1 to 13. Estrogenic activities are shown by bars, and their E2 equivalent values are given in parentheses. "A" represents a major sewage-treatment plant. A standard curve of E2 (values represent the mean ± SD) and dose–response curves of representative samples (i.e., from points 1, 2, and 7) in the YES assay are also shown.

Sampling and Concentration. Water samples were collected from 13 localities along the Lake Biwa–Yodo River system as shown in Table 1 and Figure 1 on fine days in 2002 and stored at 4 °C. Within 3 days after collection, each water sample (1 L) was filtered with a Whatman GF/C filter (Whatman International Ltd., Maidstone, England) and flowed through a Waters Sep-Pak Plus C_{18} Environment cartridge (Waters, MA) at a flow rate 10 mL/min. The cartridge was washed with 10 mL of pure water, and the bound substances were eluted from the cartridge with 2 mL of

dimethyl sulfoxide (DMSO) at a flow rate 1 mL/min and then dried by a vacuum concentrator. The extract was redissolved in 200 μL of DMSO (i.e., concentration factor was 5000) and used as a test sample in the YES assay.

Yeast Estrogenicity Screening (YES) Assay. The strain for the YES assay (*14*) carries a *LacZ* reporter plasmid, and its promoter region has estrogen responsive elements (ERE). In this assay system, the level of β-galactosidase (β-gal) activity indicates the level of human ER signaling activated by ligand binding. The assay was conducted using a previously described 96-well microtiter plate method (*14*). Briefly, 1 μL of test sample, 1.6 μL of the yeast from a 24-h culture, and 197.4 μL of growth medium containing 0.1 μg/μL of chlorophenol red-β-D-galactopyranoside (CPRG) (therefore the concentration of test sample in the assay solution became 1/200) were mixed in a well and incubated for 4–6 days at 32 °C. Then, the β-gal activity was estimated from the absorbance of the wells with a spectrophotometer at a wavelength of 540 nm. In every experiment various concentrations of E2 were assayed for making a standard curve, and using the curve the β-gal activity of each test sample was converted into E2 equivalent concentration. Since the concentration factor of the solid-phase extraction was 5000 and the dilution factor in the YES assay was 200, the E2 equivalent concentration of river water is 1/25th of that in the YES assay. The YES assay was repeated at least three times. Some of the test samples (i.e., those from sampling points 1, 2, and 7) were also diluted or concentrated and then assayed in order to make their dose–response curves.

HPLC Fractionation Analysis. HPLC fractionation of the samples was performed using a Waters 600E HPLC system equipped with an Agilent 1100 photodiode array detector and a reversed-phase column of TSK ODS-100S (ϕ 4.6 × 250 mm, TOSOH Co. Ltd., Tokyo). An aliquot (10 μL) of the extract was injected into the column and eluted over 55 min at a flow rate 1.0 mL/min with a linear gradient of 15–95% acetonitrile in 50 mM sodium acetate (pH 4.8) (*16*). The fractions were collected at 1.5-min intervals and evaporated to dryness. The dried samples were redissolved in 10 μL of DMSO and subjected to the yeast assay.

To determine retention times and UV spectra of bis(2-ethylhexyl) phthalate, daidzein, E1, E2, genistein, and *p*-*n*-nonylphenol, 5 μL of each standard (0.1 mM, in DMSO) was injected and eluted as mentioned above. After analysis of these standards, we carefully cleaned the HPLC system and checked that eluate had no β-gal activity in the YES assay.

LC–MS (Liquid Chromatograph–Mass Spectrometry) Analysis. An aliquot of the fractionated sample with strong estrogenic activity was analyzed by electrospray ionization–mass spectrometry (ESI–MS) using a Waters ZQ2000 quadrupole mass spectrometer equipped with an Agilent 1100 HPLC system. Electrospray ionization was set at 3.0 kV capillary voltage with N_2 used as the sheath gas and set at 350 L/h for desolvation gas flow and 350 °C for desolvation gas temperature. Data acquisition was performed in negative ion mode with cone voltage of 35 V with cone gas flow of 50 L/h. Ion source temperature was set at 350 °C. Electron multiplier was operated at 650 V for all analysis. The aliquot was injected into the column of Cosmosil 5C18-AR-II (ϕ 2.0 × 150 mm, Nacalai Tesque Co. Ltd., Kyoto, Japan) and eluted over 20 min at a flow rate of 0.2 mL/min with a linear gradient of 20–50% acetonitrile in 50 mM ammonium formate (pH 3.5) for 0–10 min, followed by isoclatic 50% acetonitrile in 50 mM ammonium formate (pH 3.5) for 10–20 min. With these soft-ionization conditions of LC–MS, we generally observed only parent ions of desired compounds (E2 and genistein) without remarkable degraded daughter ions, which enabled us to make an easy and sensitive identification of molecular mass of estrogenic compounds in water samples.

Quantification of Phytoestrogens in River Water. Three phytoestrogens (genistein, daizein, and genistin) in the river water were quantified by the HPLC. Each water sample (500 mL) was collected on May 20, 2003 (Table 1), and filtrated as described above. Then the filtrate was mixed with 50 mL of 1 M sodium acetate buffer (pH 5.0) and extracted with the Sep-pak Plus C_{18} Environmental cartridge as described above. The cartridge was washed with 5 mL of pure water and eluted with 5 mL of methanol followed by drying with the centrifugal concentrator. The residue was dissolved in 0.5 mL of DMSO, and a 20-μL portion was injected into the HPLC with an analytical reversed-phase column (Shim-pak FC ODS ϕ 4.6 × 150 mm (Shimadzu Co. Ltd., Kyoto, Japan)) and eluted over 15 min at a flow rate of 1 mL/min with isoclatic 20% acetonitrile in 10% (v/v) acetic acid for 0–5 min, followed by linear gradient of 20–70% acetonitrile in 10% acetic acid for 5–15 min. The phytoestrogen standards in various concentrations were also analyzed for their standard curves. The recovery of the phytoestrogens was tested by spiking 200 ng of each phytoestrogen to 500 mL of pure water, and the recovery rate was found to be 87%, 62%, and 52% for genistein, daidzein, and genistin, respectively. From the recovery rate, the area of the UV absorption peak in HPLC analysis, and the concentration factor of solid-phase extraction, we estimated the phytoestrogen concentrations in the river water.

Results and Discussion

Survey of Estrogenic Contamination in the Lake Biwa–Yodo River System. Estrogenic activities in the original water samples, calculated from the activities of concentrated water samples in the YES assay, are shown in Figure 1. The activities had an average value of 14 pmol/L (3.8 ng/L) (E2 equivalent) with a very wide range from 0 to 72 pmol/L (0–19.6 ng/L). The highest level of activity (72 pmol/L (19.6 ng/L)) was observed in the water from sampling point 2 (the Kanzaki River (Ajifu Watercourse), Osaka City), followed by the water (56 pmol/L (15.2 ng/L)) from point 7 (the Katsura River, Kyoto City). As the activity was prominent in comparison with those from the other 11 points, we analyzed these two samples further.

Identification of Estrogenic Contaminants in the Katsura River Samples. For identification of the estrogenic substance in water from sampling point 7 (the Katsura River), the concentrated samples were separated by HPLC, and fractions were collected every 1.5 min and then tested in the yeast assay. We found only a few low peaks of UV absorption throughout the HPLC chromatogram. Under these conditions of chromatography, authentic E2 and E1 known to be present in river water (*13, 17*) were eluted at 32.7 min (fraction 22) and 35.8 min (fraction 24), respectively. In the yeast assay of the HPLC fractions, strong estrogenic activities were detected in fractions 22 and 24 whose retention times were the same as those of E2 and E1, but no UV absorption peaks corresponding to the fractions were observed (data not shown). Sampling point 7 is located just downstream of a sewage-treatment plant (effluent: 600 000 m^3/day, area population: 770 000 persons, denoted as A in Figure 1). From the amount of flowing river water and the volume of the effluent at this sampling point, 30% of the river water is estimated to be of effluent origin (*13*). Sewage-treatment plants are known to be the major source of E1 and E2 (i.e., human/animal urine origin) in river water (*15–20*). In the Katsura River, an administrative agency's survey detected E1 and E2 with comparable concentrations to ours using an enzyme-linked immunosorbent assay and concluded that the major source is effluent from the sewage-treatment plant (*13*). From the data showing that estrogenic activity in the YES assay corresponded to the fractions where E1 and E2 are known to elute, we concluded that these natural estrogens

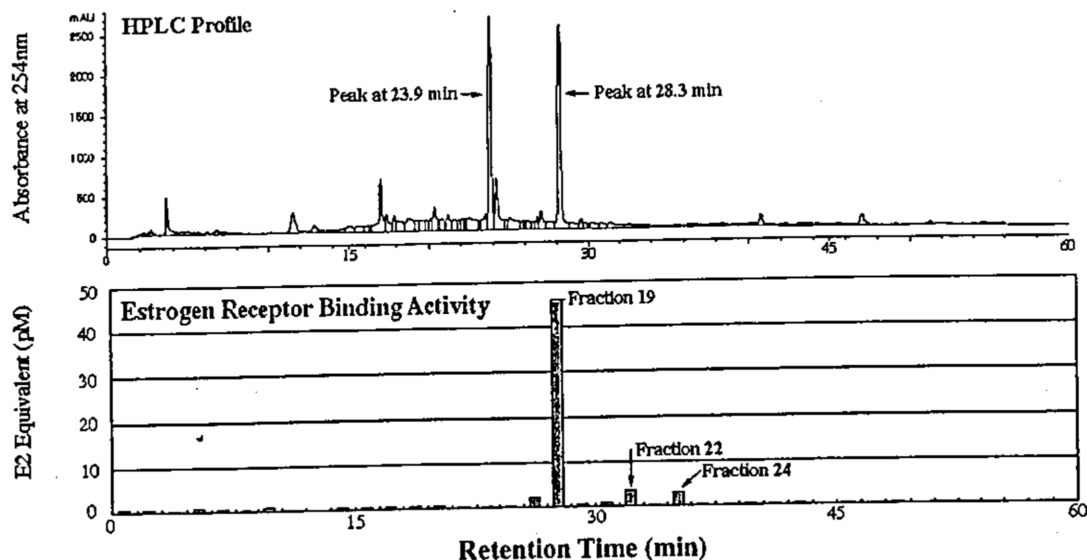

FIGURE 2. HPLC profile and estrogenic activity of the HPLC fractions of the sample from point 2. The UV absorbance and estrogenic activity are shown in the upper and lower panels, respectively. The value of the E2 equivalent is converted to be comparable with that in Figure 1. An estrogenic substance (genistein) was eluted at a retention time of 28.3 min as a single peak corresponding to fraction 19. The on-line UV spectrum of the peak is shown as panel A in Figure 3. A single peak of UV absorption at 23.9 min corresponds to daidzein. Weak estrogenic activities of fractions 22 and 24 would be due to E2 and E1, respectively.

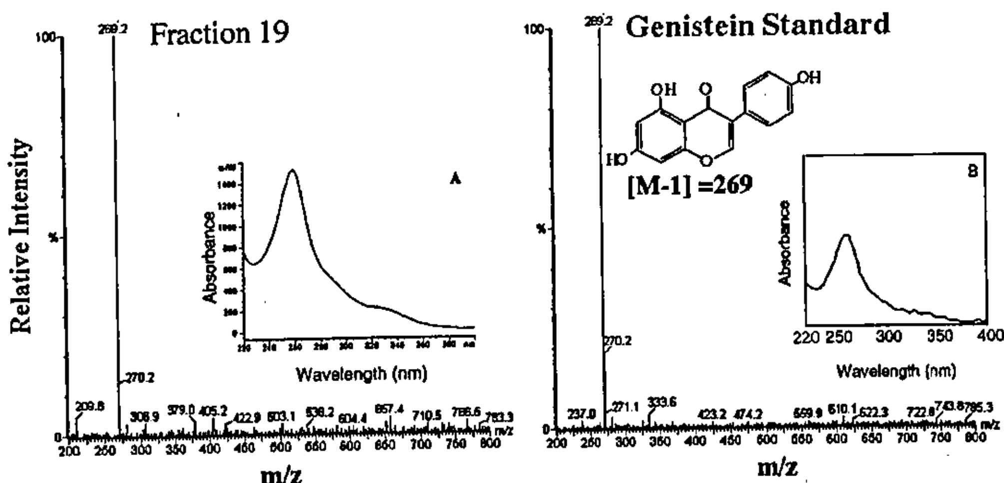

FIGURE 3. ES–MS and UV absorption spectra (A and B) of fraction 19 (left) and a genistein standard (right). The chemical structure of genistein is also given in the right panel. The UV absorption spectrum of a genistein standard (B) is from Fukutake et al. (25).

were responsible for the estrogenic activity in the water samples. However, without positive identification of these compounds using more sensitive analytical techniques (i.e., LC–MS/MS), we cannot be certain that E1 and E2 were responsible for the estrogenic activity in this water sample.

Identification of an Estrogenic Contaminant in the Kanzaki River Sample. For identification of the estrogenic substance in water from sampling point 2 (the Kanzaki River), the concentrated samples were separated by HPLC, and fractions were collected every 1.5 min and then subjected to the yeast assay. As shown in Figure 2, the HPLC chromatogram contained two major peaks of UV absorption (retention times 23.9 and 28.3 min), and the peak at 28.3 min, corresponding to fraction 19 (27.0–28.5 min), showed strong estrogenic activity in the yeast assay. This activity contributed to 65% of the estrogenic activity of the sample. This peak corresponded to neither bis(2-ethylhexyl) phthalate nor *p-n*-nonylphenol, which had been detected at this sampling point by the municipal government (*21*). Two other fractions having weak estrogenic activities with no UV absorption were also detected at 32.7 min (fraction 22) and 35.8 min (fraction 24), which would be due to E2 and E1, respectively.

For structural determination of the estrogenic substance in sample 2 (the Kanzaki River), we further analyzed HPLC fraction 19 of the sample by LC–MS. As shown in Figure 3, the parent ion of the compound in the fraction was *m/z* 269 $[M-1]^-$, being identical to a putative parent ion of genistein, which is an isoflavone contained in soybean and is known to have estrogenic activity. Then a genistein standard was subjected to LC–MS analysis. Fraction 19 and a genistein standard were eluted at 11.7 and 11.8 min, respectively, and both parent mass ions were confirmed to be identical. Furthermore, the fraction 19 and a genistein standard had the same retention time and the identical UV absorption spectrum in other HPLC conditions. We therefore safely conclude that fraction 19 contains genistein.

From the area of the UV absorption peak corresponding to fraction 19 (Figure 2), we estimated the concentration of genistein in the river water at 24.0 μg/L and its E2 equivalent concentration at 35.5 pM since the relative potency of ER binding of genistein is 4.0×10^{-4} (as that of E2 is 1.0) (*22*). The other major peak of UV absorption (at 23.9 min in HPLC Profile) in Figure 2 was a phytoestrogen daidzein since its retention time and UV spectrum were identical with those

of daidzein standard (identification data are not shown here). The relative ER-binding potency of daidzein is very weak (2.0×10^{-6}) (*22*), so that we could not detect reporter gene activity in Figure 2.

Genistein is one of the most abundant phytoestrogens present in soybean seeds, flour, and many vegetables (*23, 24*). Soybean products such as tofu (bean curd) and soymilk and fermented soybean products (e.g., Japanese miso and natto) also contain genistein (*25, 26*). Logana et al. detected genistein in the Italian river Tiber at the concentration of 4–7 ng/L (*27*).

Concentration of Phytoestrogens in the Kanzaki River. We measured the concentration of three phytoestrogens (genistein, daizein, and genistin) at sampling point 2 on another day (Table 1). The concentrations of genistein and daidzein were 143.4 and 42.9 μg/L, respectively. Genistin was not detected (<0.4 μg/L). This concentration of genistein may be biologically significant. Scholz et al. (*28*) reported that 6-month-old male Japanese killifish medaka (*Oryzias latipes*) exposed to 10 μg/L of genistein for 4 weeks strongly induced vitellogenin (VTG) synthesis. Kiparissis et al. (*29*) reported that waterborne exposure of Japanese medaka to genistein from soon after hatch to 100 days posthatch induced various gonadal abnormalities, and many of these gonadal abnormalities were induced by 1 μg/L of genistein. Intraperitoneal injection of genistein produced estrogenic responses in a Japanese medaka (*30*). Bennetau-Pelissero et al. (*31*) reported accelerated testicular development and delayed spawning in rainbow trout (*Oncorhynchus mykiss*) that fed on genistein-enriched diets for 1 year. Estrogenic effects of genistein were also reported in rats and mice (*32–36*). On the other hand, genistein has been thought to have an important role in reducing the incidence of human breast and prostate cancers (*36–39*).

It is surprising that such a high concentration of phytoestrogens were detected in river water. Sampling point 2 is a residential quarter in Osaka City where small and medium-sized industrial factories of many types lie scattered. There are some possible dischargers including food and wood pulp factories. The genistein concentration of an untreated effluent from a Indonesian tofu (soybean curd) industry were 930 μg/L (Ermawati et al., unpublished data). On the other hand, Kiparissis et al. (*40*) reported that wood pulp and pulp mill effluent contains 30 μg/kg and 13 μg/L of genistein, respectively, in Canada.

For the moment, we have not identified the origin of genistein. Furthermore, we could not detect the binding activity of genistein in the river 2 km downstream (Aikawa, Higashiyodogawa Ward, Osaka City) from point 2 (data not shown). Dilution would be a major cause of the disappearance, although genistein may transfer from water to detritus quickly due to its hydrophobicity or may be decomposed in the environment easily. To evaluate the ecotoxicity of genistein and environmental safety of Kanzaki River water, more studies are required.

Acknowledgments

The strain for the YES assay was kindly supplied to T. Matsuda by Professor J. P. Sumpter (Brunel University, Uxbridge, UK). This work was supported in part by Grants-in-aid for Scientific Research B (No. 14380257) and for Scientific Research on Priority Areas (Nos. 13,027,279 and 14,042,258) from the Japanese Ministry of Education, Science, Sports and Culture and by the River Environment Funds (Nos. 13-1-1-22 and 15-1-1-21) in charge of the Foundation of River and Watershed Environment Management (FOREM), Japan. This work was also supported in part by funds under a contract with the Ministry of Environment of Japan and the Promotion and Mutual Aid Corporation for Private Schools of Japan.

Literature Cited

(1) Maruoka, S.; Yamaoka, S. *Mutat. Res.* **1982**, *102*, 13–26.
(2) Sayato, Y.; Nakamuro, K.; Ueno, K.; Goto, R. *Mutat. Res.* **1993**, *300*, 207–213.
(3) Sakamoto, H.; Hayatsu, H. *Bull. Environ. Contam. Toxicol.* **1990**, *44*, 521–528.
(4) Ohe, T.; Takeuchi, N.; Watanabe, T.; Tada, A.; Nukaya, H.; Terao, Y.; Sawanishi, H.; Hirayama, T.; Sugimura, T.; Wakabayashi, K. *Environ. Health Perspect.* **1999**, *107*, 701–704.
(5) Shiozawa, T.; Tada, A.; Nukaya, H.; Watanabe, T.; Takahashi, Y.; Asanoma, M.; Ohe, T.; Sawanishi, H.; Katsuhara, T.; Sugimura, T.; Wakabayashi, K.; Terao, Y. *Chem. Res. Toxicol.* **2000**, *13*, 535–540.
(6) Watanabe, T.; Nukaya, H.; Terao, Y.; Takahashi, Y.; Tada, A.; Takamura, T.; Sawanishi, H.; Ohe, T.; Hirayama, T.; Sugimura, T.; Wakabayashi, K. *Mutat. Res.* **2001**, *498*, 107–115.
(7) Watanabe, T.; Shiozawa, T.; Takahashi, Y.; Takahashi, T.; Terao, Y.; Nukaya, H.; Takamura, T.; Sawanishi, H.; Ohe, T.; Hirayama, T.; Wakabayashi, K. *Mutagenesis* **2002**, *17*, 293–299.
(8) Colborn, T., Clement, C., Eds. *Chemically-Induced Alternations in Sexual and Functional Development: The Wildlife/Human Connection*; Advances in Modern Environmental Toxicology 21; Princeton Scientific: Princeton, NJ, 1992.
(9) Bitman, J.; Cecil, H. C. *J. Agric. Food Chem.* **1970**, *18*, 1108–1112.
(10) Nelson, J. A.; Struck, R. F.; James, R. *J. Toxicol. Environ. Health* **1978**, *4*, 325–339.
(11) Soto, A. M.; Lin, T. M.; Justicia, H.; Silvia, R. M.; Sonnenschein, C. In *Chemically-Induced Alternations in Sexual and Functional Development: The Wildlife/Human Connection*; Colborn, T., Clement, C., Eds.; Advances in Modern Environmental Toxicology 21; Princeton Scientific: Princeton, NJ, 1992; pp 295–309.
(12) Jobling, S.; Sumpter, J. P. *Aquat. Toxicol.* **1993**, *27*, 361–372.
(13) Ministry of Land, Infrastructure and Transport, Government of Japan. *Mizukankyo ni okeru naibunpikakuran busshitsu nikansuru zittai chosa kekka (Survey Results of Endocrine Disrupting Chemicals in the Water Environment)* Ministry of Land, Infrastructure and Transport, Government of Japan: Tokyo, 2001 (in Japanese)
(14) Routledge, E. J.; Sumpter, E. J. *Environ. Toxicol. Chem.* **1996**, *15*, 241–248.
(15) Desbrow, C.; Routledge, E. J.; Brighty, G. C.; Sumpter, J. P.; Waldock, M. *Environ. Sci. Technol.* **1998**, *32*, 1549–1558.
(16) Matsui, S.; Lee, B.-C.; Kawami, F.; Shimizu, S.; Matsuda, T. *Lakes Reservoirs* **2002**, *7*, 289–293.
(17) Tyler, C. R.; Routledge, E. J. *Pure Appl. Chem.* **1998**, *70*, 1795–1804.
(18) Matsui, S.; Takigami, H.; Matsuda, T.; Taniguchi, N.; Adachi, J.; Kawami, H.; Shimizu, S. *Water Sci. Technol.* **2000**, *42*, 173–179.
(19) Shishida, K.; Echigo, S.; Kosaka, K.; Tabasaki, M.; Matsuda, T.; Takigami, H.; Yamada, H.; Shimizu, Y.; Matsui, S. *Environ. Technol.* **2000**, *21*, 553–360.
(20) Takigami, H.; Taniguchi, N.; Matsuda, T.; Yamada, M.; Shimizu, Y.; Matsui, S. *Water. Sci. Technol.* **2000**, *42*, 45–51.
(21) Osaka Prefecture. *Kankyo Hakusyo (Quality of the Environment; White paper)* Osaka Prefecture: Osaka, 2002 (in Japanese).
(22) Nakamuro, K.; Ueno, H.; Okuno, T.; Sakazaki, H.; Kawai, H.; Kamei, T.; Ugawa, M. *J. Jpn. Soc. Water Environ.* **2002**, *25*, 355–360.
(23) Farnsworth, N. R.; Bingel, A. S.; Cordell, A.; Crane, F. A.; Fong, H. H. S. *J. Pharm. Sci.* **1975**, *64*, 717–754.
(24) Setchell, K. D. R. *Am. J. Clin. Nutr.* **1998**, *68*, 1333S–1346S.
(25) Fukutake, M.; Takahashi, M.; Ishida, K.; Kawamura, H.; Sugimura, T.; Wakabayashi, K. *Food Chem. Toxicol.* **1996**, *34*, 457–461.
(26) Takamura-Enya, T.; Ishihara, J.; Tahara, S.; Goto, S.; Totsuka, Y.; Sugimura, T.; Wakabayashi, K. *Food Chem. Toxicol.* **2003**, *41*, 543–550.
(27) Logana, A.; Bacoloni, A.; De Leva, I.; Faberi, A.; Fago, G.; Marino, A. *Anal. Chim. Acta* **2004**, *501*, 79–88.
(28) Scholz, S.; Kordes, C.; Hamann, J.; Gutzeit, H. O. *Mar. Environ. Res.* **2004**, *57*, 235–244.
(29) Kiparissis, Y.; Balch, G. C.; Metcalfe, T. L.; Metcalfe, C. D. *Environ. Health Perspect.* **2003**, *111*, 1158–1163.
(30) Zhang, L.; Khan, I. A.; Foran, C. M. *Comp. Biochem. Physiol. Part C* **2002**, *132*, 203-211.
(31) Bennetau-Pelissero, C.; Breton, B. B.; Bennetau, B.; Corraze, G.; Le Menn, F.; Davail-Cuisset, B.; Helou, C.; Kaushik, S. J. *Gen. Comp. Endocrinol.* **2001**, *121*, 173–187.

(32) Levy, J. R.; Faber, K. A.; Ayyash, L.; Hughs, C. L. *Proc. Soc. Exp. Biol. Med.* **1995**, *208*, 60–66.
(33) Santell, R. C.; Chang, Y. C.; Nair, M. G.; Helferich, W. G. *J. Nutr.* **1997**, *127*, 263–269.
(34) Strauss, L.; Makela, S.; Joshi, S.; Huhtaniemi, I.; Santti, R. *Mol. Cell. Endocrinol.* **1998**, *144*, 83–93.
(35) Casanova, M.; You, L.; Gaido, K. W.: Archibeque-Engle, S.; Janszen, D. B.; Heck, H. A. *Toxicol. Sci.* **1999**, *51*, 236–244.
(36) Barnes, S.; Peterson, G.; Grubbs, C.; Setchell, K. *Adv. Exp. Med. Biol.* **1994**, *354*, 135–147.
(37) Peterson, G.; Barnes, S. *Prostate* **1993**, *22*, 335–345.
(38) Peterson, G.; Barnes, S. *Biochem. Biophys. Res. Commun.* **1991**, *179*, 661–667.
(39) Yatani, R.; Chigusa, I.; Akazaki, K.; Stemmermann, G. N.; Welsh, R. A.; Correa, P. *Int. J. Cancer* **1982**, *29*, 611–616.
(40) Kiparissis, Y.; Hughes, R.; Metcalfe, C.; Ternes, T. *Environ. Sci. Technol.* **2001**, *35*, 2423–2427.

Received for review February 16, 2004. Revised manuscript received June 7, 2004. Accepted July 2, 2004.

ES049764V

Suppressive function of androgen receptor in bone resorption

Hirotaka Kawano*†‡, Takashi Sato*‡§, Takashi Yamada*†, Takahiro Matsumoto*§, Keisuke Sekine*, Tomoyuki Watanabe*, Takashi Nakamura*, Toru Fukuda*, Kimihiro Yoshimura*, Tatsuya Yoshizawa*, Ken-ichi Aihara*, Yoko Yamamoto*, Yuko Nakamichi*, Daniel Metzger¶, Pierre Chambon¶, Kozo Nakamura†, Hiroshi Kawaguchi†, and Shigeaki Kato*§‖

*Institute of Molecular and Cellular Biosciences and †Department of Orthopedic Surgery, Faculty of Medicine, University of Tokyo, 1-1-1 Yayoi, Bunkyo-ku, Tokyo 113-0032, Japan; §Solution-Oriented Research for Science and Technology, Japan Science and Technology Corporation, 4-1-8 Honcho, Kawaguchi, Saitama 332-0012, Japan; and ¶Institut de Génétique et de Biologie Moleculaire et Cellulaire, Centre National de la Recherche Scientifique, Institut National de la Santé et de la Recherche Médicale, Université Louis Pasteur, Collège de France, 67404 Illkirch, Strasbourg, France

Contributed by Pierre Chambon, June 6, 2003

As locally converted estrogen from testicular testosterone contributes to apparent androgen activity, the physiological significance of androgen receptor (AR) function in the beneficial effects of androgens on skeletal tissues has remained unclear. We show here that inactivation of AR in mice using a Cre-loxP system-mediated gene-targeting technique caused bone loss in males but not in females. Histomorphometric analyses of 8-week-old male AR knockout (ARKO) mice showed high bone turnover with increased bone resorption that resulted in reduced trabecular and cortical bone mass without affecting bone shape. Bone loss in orchidectomized male ARKO mice was only partially prevented by treatment with aromatizable testosterone. Analysis of primary osteoblasts and osteoclasts from ARKO mice revealed that AR function was required for the suppressive effects of androgens on osteoclastogenesis supporting activity of osteoblasts but not on osteoclasts. Furthermore, expression of the receptor activator of NF-κB ligand (*RANKL*) gene, which encodes a major osteoclastogenesis inducer, was found to be up-regulated in osteoblasts from AR-deficient mice. Our results indicate that AR function is indispensable for male-type bone formation and remodeling.

Steroid sex hormones are essential for normal skeletal development and maintenance of healthy bone remodeling during adult life (1, 2). Sex hormone status reflects bone mass, such that hormonal deficiency is well known to lead to progressive bone loss (3). The most striking example, osteoporosis in postmenopausal women, is a state of estrogen deficiency coupled with imbalanced bone remodeling, with higher bone resorption than bone formation, and can be rescued by estrogen replacement (4). Although androgens seem to exert beneficial effects in both males and females (3, 5), the physiological role of the androgen–androgen receptor (AR) system in skeletal tissues has not yet been well established. This is because estrogens are locally converted from serum androgens by aromatase present in bone and seem to contribute to the overt androgen effects on the skeleton (5, 6). This concept is supported by observations that male mice deficient in either aromatase or skeletal major estrogen receptor (ERα) suffer bone loss (6, 7). However, a number of studies have demonstrated that androgen treatment is protective against bone loss caused by the impaired estrogen signaling (3, 5), raising the possibility that AR-mediated androgen effects in bone remodeling are physiologically significant and independent of estrogen actions.

AR is a member of the nuclear steroid/thyroid hormone receptor gene superfamily and acts as a ligand-inducible transcription factor (8, 9). Most androgen effects are thought to be exerted through the transcriptional control of particular sets of target genes by AR. Upon hormone binding, AR is translocated from the cytosol into the nucleus and binds specific promoter elements. A number of coregulators and/or coregulator complexes are then recruited to AR, which then activates or represses the transcription of various target genes (10–13). Like the well described target tissues for androgens, bone tissues also express AR, being present in both osteoblasts and osteoclasts (2). Reflecting this AR expression, androgens have been shown to regulate the expression of several genes encoding growth factors and cytokines that control bone remodeling via both osteoblasts and osteoclasts (2). However, the role of AR in bone cell gene expression has not been well studied because of the lack of animals and cell lines deficient in AR expression.

To define the physiological functions of AR in target tissues, an AR-null mutant mouse line was generated by means of the Cre–loxP system, which was used to circumvent the problem of male infertility (14). The present study found that 8-week-old male AR knockout (ARKO; $AR^{L-/Y}$) mice developed osteopenia and exhibited retarded growth curves, although normal bone shape was retained and overt phenotypes were indistinguishable from those of WT female littermates. Although high bone turnover, with more bone resorption than formation, was seen in 8-week-old $AR^{L-/Y}$ male mice, female ARKO ($AR^{L-/L-}$) mice seemed normal with respect to bone mass and bone remodeling. These findings suggest that AR function was essential for male-type bone mass and bone remodeling. Furthermore, up-regulation of receptor activator of NF-κB ligand (*RANKL*) gene expression, along with enhanced potency to induce osteoclastogenesis in an *in vitro* coculture system, was observed for AR-deficient osteoblasts. Taken together, our results indicate that AR performs a suppressive function in osteoblasts during osteoclastogenesis that is indispensable for normal male-type bone formation and remodeling.

Materials and Methods

Animals. ARKO mice with the original C57BL6/CBA hybrid background were generated and maintained as reported (14). All mice were maintained according to the protocol approved by the Animal Care and Use Committee of the University of Tokyo.

Identification of AR Transcript by RT-PCR. Total mRNA was extracted from excised femora and tibiae by using an Isogen kit (Wako Pure Chemical, Osaka) and reverse transcribed by using XL reverse transcriptase (Takara Shuzo, Otsu, Japan) and an oligo(dT) primer (Takara Shuzo). After first-strand cDNA synthesis, 5% of the reaction mixture was amplified with r-*Taq*DNA polymerase (Takara Shuzo) by using specific primer pairs: 5′-CATGTAGGCCATGAGGTCCACCAC-3′ and 5′-TGAAGGTCGGTGTGAACGGATTTGGC-3′ for G3PDH;

Abbreviations: AR, androgen receptor; ARKO, AR knockout; ER, estrogen receptor; BMD, bone mineral density; DHT, 5α-dehydrotestosterone; RANKL, receptor activator of NF-κB ligand; TRAP, tartrate-resistant acid phosphatase; M-CSF, macrophage colony-stimulating factor.

‡H.K. and T.S. contributed equally to this work.

‖To whom correspondence should be addressed. E-mail: uskato@mail.ecc.u-tokyo.ac.jp.

www.pnas.org/cgi/doi/10.1073/pnas.1533500100

5′-TGGTAGCTGGTACTTCTAATGC-3′ and 5′-CATAAG-GTCCGGAGTAGTTCTC-3′ for AR-1; and 5′-CAGAAG-TATCTATGTGCCAG-3′ and 5′-ATCTTCTGGGATGGGTC-CTCAG-3′ for AR-2. Up to 35 cycles of amplification were performed, with each cycle consisting of 96°C for 30 s, 55°C for 60 s, and 72°C for 60 s.

Analysis of Skeletal Morphology. Bone radiographs of excised femora and tibiae from 8-week-old WT and ARKO littermates were taken by using a soft x-ray apparatus (CMB-2; Softex, Tokyo). Three-dimensional computed tomography scanning was performed by using a composite x-ray analyzing system (NX-HCP; NS-ELEX, Tokyo). Bone mineral density (BMD) was measured by dual energy x-ray absorptiometry using a bone mineral analyzer (Piximus densitometer; Lunar, Madison, WI). Skeletal preparations for morphology were performed as described (15). Trabecular bone parameters were measured in an area 1.2 mm in length from 0.1 mm below the growth plate at the proximal metaphysis of tibiae, and cortex bone parameters were measured at the midshaft of femora.

Orchidectomy and Hormone Replacement. Male WT and ARKO littermates were orchidectomized or sham operated at 3 weeks of age and implanted s.c. with a slow-releasing pellet (10 mg/60 days) (Innovative Research of America) of placebo, testosterone (T), or 5α-dehydrotestosterone (DHT). BMD of femora was compared among eight experimental groups at 8 weeks of age.

Measurement of Serum Bone Metabolic Markers. Serum osteocalcin and urinary deoxypyridinoline were measured as bone formation and resorption markers in male WT and ARKO mice. Blood was sampled at time of death, and urine was collected for 24 h before death by using oil-sealed bottles in metabolic cages (Kurea, Tokyo). Concentration of deoxypyridinoline was corrected according to urinary creatinine concentration.

Statistical Analysis. Group means were compared by ANOVA, and the significance of differences were determined by post hoc testing with Bonferroni's method.

***Ex Vivo* Osteoblast Cultures.** Osteoblast cultures were performed as described (15). For the cell proliferation assay, primary osteoblasts were inoculated at a density of 2×10^3 cells per well in a 96-multiwell plate for 2 days, and cell number was counted with cell-counting kit solution (Wako Pure Chemical) according to the manufacturer's protocol. For the measurement of alkaline phosphatase activity, primary osteoblasts were inoculated at a density of 5×10^4 cells per 24 multiwells and cultured in αMEM containing 10% FBS and 50 μg/ml ascorbic acid. After 14 days of culture, alkaline phosphatase activity in the cell lysate was measured by using a Wako ALP kit (Wako Pure Chemical).

Osteoclastogenesis in Coculture of Bone Marrow Cells and Osteoblasts. To visualize osteoclasts, staining for tartrate-resistant acid phosphatase (TRAP) activity is widely used (15). TRAP-positive multinucleated osteoclasts were generated from hemopoietic cells by coculturing with osteoblasts. As a source of hemopoietic cells, bone marrow cells (5×10^5 cells per well) and osteoblasts (5×10^4 cells per well) were isolated and placed in 0.5 ml per 24 multiwells of αMEM/10% FBS for 8 days in the presence of 10 nM 1α,25(OH)$_2$D$_3$ (16). To determine osteoclast survival, osteoclasts were isolated and cultured as described (15). The number of TRAP-positive and trypan blue-negative multinucleated cells were counted at 0, 12, 18, 24, and 48 h. Bone resorption activity was measured as described (15).

Osteoclastogenesis in Bone Marrow Cell Culture. Bone marrow cells were inoculated at a density of 5×10^5 cells per 24 multiwells and cultured in 1.0 ml per 24 multiwells of αMEM/10% FBS with 100 ng/ml macrophage colony-stimulating factor (M-CSF) for the first 48 h, after which 100 ng/ml M-CSF and 100 ng/ml RANKL were added and incubated for an additional 96 h. TRAP-positive multinucleated osteoclasts were then counted.

RT-PCR Analysis of *RANKL* Gene Expression. Semiquantitative RT-PCR was carried out on primary cultured osteoblasts for a number of osteoblastic factor genes (17). After osteoblasts were cultured to confluency in αMEM containing 10% FBS, 1α,25(OH)$_2$D$_3$ (10 nM) was added with DHT (10 nM) or vehicle and cultured for 48 h. Total RNA extraction and reverse transcription was performed as described above. After first-strand cDNA synthesis, 5% of the reaction mixture was amplified with r-*Taq*DNA polymerase (Takara Shuzo) by using specific primer pairs 5′-GCATCGCTCTGTTCCTGTA-3′ and 5′-GTGCTCCCTCCTTTCATCA-3′ for RANKL and G3PDH. Up to 25 cycles of amplification were performed, with each cycle consisting of 96°C for 30 s, 55°C for 60 s, and 72°C for 60 s.

Results

Male ARKO Mice Exhibit Abnormalities Typical of Testicular Feminization Mutant Rodents. To avoid male infertility caused by AR mutation, thereby preventing the establishment of a line of AR-deficient mice, we applied the Cre-loxP system to first flox the *AR* gene on the sole X chromosome in male mice (14). Floxed male mice (AR$^{L3/Y}$) (Fig. 1*a*) seemed completely normal with regard to bone mass and reproduction and showed no apparent differences from WT littermates. Male ARKO (AR$^{L-/Y}$) mice, descended from female AR heterozygotes (AR$^{+/L-}$), showed growth retardation compared with male littermates, but growth curves and external reproductive organs were indistinguishable from those of female littermates up to 8 weeks of age (Fig. 1*b*). Reflecting the atrophic testis in 8-week-old AR$^{L-/Y}$ mice, testicular androgen production seemed to be severely impaired, leading to marked reduction in serum gonadal androgen levels, whereas serum estrogen and adrenal androgen levels remained unchanged (Fig. 1*c*). Thus, the phenotypic abnormality of AR$^{L-/Y}$ mice seemed identical to that reported for testicular feminization mutant rodents, natural mutants with AR dysfunction (3, 10). To our surprise, female ARKO (AR$^{L-/L-}$), which never exist in nature, exhibited no phenotypic abnormality up to 8 weeks of age. However, it was possible that the abnormal AR protein derived from the genetically mutated AR gene locus still retained some level of androgen responsiveness (18). To address this issue, the presence of AR transcripts in bone in both male (AR$^{L-/Y}$) and female (AR$^{L-/L-}$) ARKO mice was assessed. No transcripts were detected by Northern blotting (data not shown) or by RT-PCR using several primer pairs performed on total bone tissue (Fig. 1*d*). These findings established that our ARKO mouse was indeed a mammalian AR-null mutant model.

Osteopenia in Male ARKO Mice. To examine the physiological roles of AR in mediating androgenic effects on bone tissue, we first analyzed the skeletal morphology of AR$^{L-/Y}$ mice. Soft x-ray analysis revealed severe osteopenia of femora and tibiae from 8-week-old male mice (Fig. 1*e*), but also that bone shape and bone length (Figs. 1*e* and 2*b*) were not affected by AR inactivation. This was consistent with the clear loss in radiographic BMD of femora from AR$^{L-/Y}$ mice compared with WT male littermates. The BMD of AR$^{L-/Y}$ mice was even lower than that of WT female littermates (Fig. 2*a*). Three-dimensional computed tomography scan analysis of femora showed that bone loss in AR$^{L-/Y}$ mice occurred throughout the entire femur (Fig. 2*c*). Histomorphometric analysis of proximal tibiae from AR$^{L-/Y}$ mice confirmed that trabecular bone volumes (bone volume per tissue volume: BV/TV) were markedly decreased, whereas no overt differences in growth plates were detected between

GENETICS

Fig. 1. (a) Strategy to generate male and female ARKO mice using CMV-Cre transgenic mice. (b) Growth curves of ARKO and WT littermate mice. (c) Serum hormone levels in 8-week-old ARKO and WT mice. (d) Lack of AR expression in bone of ARKO mice (RT-PCR). (e) Soft x-ray images of femora and tibiae from 8-week-old ARKO and WT mice.

$AR^{L-/Y}$ and WT mice (Fig. 2*d*). Such bone loss was also evident in cortical bones as estimated by cortex thickness (Fig. 2*e*). In contrast, no clear loss of bone mass was detected in female ARKO mice (Figs. 1*e* and 2*a*). Together, these findings suggest that $AR^{L-/Y}$ mice developed osteopenia, which implies that the AR function is required for male-type bone mass and remodeling.

The Suppressive Function of AR in Bone Resorption Is Abrogated in Male ARKO Mice. To further study the process of bone loss in $AR^{L-/Y}$ mice, bone remodeling was assessed. The bone formation rate of the trabecular bone was directly estimated by calcein double-labeling of the mineralized matrix (17). Unexpectedly, the bone formation parameters (Ob.S/BS and MAR) were significantly increased in $AR^{L-/Y}$ mice, with increased thickness of the region between the two calcein-labeled layers compared with WT littermates (Fig. 3*a*). This increased bone formation was also found in the cortical bone, in the endocortical area of the axial section (Fig. 3*b*). We observed an increase in the number of TRAP-positive mature osteoclasts (Fig. 3*c*). This was reflected in the significantly increased bone resorption parameters (Oc.S/BS, N.Oc/B.Pm) (Fig. 3*c*). Our finding of enhanced bone turnover was further supported by the increased levels of serum osteocalcin and urinary deoxypyridinoline (Fig. 3*d*). Although female ARKO mice exhibited no abnormal bone remodeling, our findings suggested that AR inactivation caused high turnover bone remodeling with higher bone resorption than formation, resulting in the development of osteopenia in males.

Effects of Androgens Other Than Those from Locally Converted Estrogen on Male Bone Remodeling. It is thought that estrogen converted from serum testosterone by aromatase expressed in androgen target tissues, including bone, contributes to apparent androgen activity (6). As serum testosterone levels were drastically decreased due to atrophic testes in $AR^{L-/Y}$ mice, it was impossible to exclude the possibility that the osteopenia in $AR^{L-/Y}$ mice simply reflected the impaired action of converted estrogen from serum testosterone on skeletal tissues. To address this issue, aromatizable testosterone (T) and nonaromatizable androgen DHT were given to orchidectomized $AR^{L-/Y}$ and WT littermates, and the femur BMD was assessed. Whereas orchidectomy caused no further BMD loss in $AR^{L-/Y}$ femora, BMD values from orchidectomized WT littermates were higher, but not significantly, than those of $AR^{L-/Y}$ mice (Fig. 3*e*). Also, whereas T, but not DHT, effectively recovered BMD, the recovery in $AR^{L-/Y}$ mice due to T was only ≈50% of that in intact males (Fig. 3*e*), which suggests that androgen actions mediated via AR are significant in protecting against bone loss.

Suppressive Effects of AR on *in Vitro* Osteoclastogenesis and *RANKL* Gene Expression in Osteoblasts. To further explore the mechanisms of increased bone resorption in $AR^{L-/Y}$ mice, *in vitro* osteoclas-

PNAS PNAS PNAS PNAS

Fig. 2. Osteopenia in male ARKO mice. (*a*) Bone loss in femur of 8-week-old male ARKO mice by BMD analysis. (*b*) Bone length in 8-week-old ARKO and WT littermate mice. (*c*) Three-dimensional computed tomography images of distal femora and axial sections of distal metaphyses from representative 8-week-old male WT and ARKO littermates. (*d*) Histological features and histomorphometry of the proximal tibiae from 8-week-old male ARKO and WT mice. For Villanueva–Goldner staining of sections from representative ARKO and WT male littermates, mineralized bone is stained green. BV/TV, trabecular bone volume expressed as a percentage of total tissue volume. (*e*) Histological features and histomorphometry of the midshaft of femora of 8-week-old mice. Cort.Th., cortex thickness.

Fig. 3. High bone turnover in male ARKO mice and its partial prevention by an aromatizable androgen. (*a*) Two calcein-labeled mineralized fronts visualized by fluorescent micrography and bone formation parameters in the proximal tibia of 8-week-old male ARKO and WT littermate mice. Ob.S/BS, percentage of bone surface covered by cuboidal osteoblasts; MAR, mineral apposition rate. (*b*) Two calcein-labeled mineralized fronts and bone histomorphometric parameters in the midshaft of femora from 8-week-old male ARKO and WT littermate mice. ES/BS, percentage of eroded surface. (*c*) TRAP staining and bone resorption parameters in the proximal tibiae of 8-week-old male WT and ARKO mice. TRAP-positive osteoclasts on secondary spongiosa are stained red. Oc.S/BS, percentage of bone surface covered by mature osteoclasts; N.Oc/B.Pm, number of mature osteoclasts in 10 cm of bone perimeter. (*d*) Serum osteocalcin levels and urinary deoxypyridinoline levels of 8-week-old male ARKO and WT mice. (*e*) BMD values of femora from 8-week-old mice after orchidectomy (ORX) and hormone replacement. T, testosterone.

togenesis was assessed using osteoclast precursor cells from bone marrow and calvaria osteoblasts (16, 17) derived from male WT and $AR^{L-/Y}$ mice (Fig. 4*a*). TRAP-positive multinucleated osteoclasts were clearly cytodifferentiated by $1\alpha,25(OH)_2D_3$ stimulation even when AR was absent in osteoclast precursor cells (Fig. 4*a*). *RANKL* is a member of tumor necrosis factor-α superfamily cytokines, which induces osteoclastogenesis and activates osteoclast function. Consistent with normal osteoclastogenesis in response to $1\alpha,25(OH)_2D_3$, RANKL signaling activated by RANKL and M-CSF during osteoclastogenesis also seemed unaffected in AR-deficient osteoclasts (Fig. 4*c*). Moreover, resorption pits produced by cultured AR-deficient primary osteoclasts seemed normal both in terms of numbers and area when compared with osteoclasts from WT littermates (Fig. 4*b*). Surprisingly, the survival rate of osteoclasts in the presence of DHT was unaffected by AR inactivation (Fig. 4*d*), in sharp contrast to a recent report concerning the osteoclast survival function of AR (19). However, AR inactivation in osteoblasts seemed to potentiate osteoblastic functions that promote osteoclastogenesis in the presence of inducers (Fig. 4 *a* and *b*). However, we detected no abnormalities in cultured AR-deficient primary osteoblast cell proliferation by MTT [3-(4,5-dimethylthiazol-2-yl)-2,5-diphenyl tetrazolium bromide] assay or maturation by alkaline phosphatase activity (data not shown). In searching for the osteoblastic factor responsible for the increased osteoclastogenesis (20, 21), *RANKL* turned out to be transcriptionally up-regulated in AR-deficient osteoblasts (Fig. 4*e*). Thus, our findings suggest that the suppressive function of AR on *RANKL* gene expression mediates the protective effects of androgen on bone remodeling through the inhibition of bone resorption.

Fig. 4. (*a*) Osteoclastogenesis in bone marrow cell and osteoblast cocultures. TRAP-positive multinucleated osteoclast numbers were counted after 8-day coculture of bone marrow cells and osteoblasts from male ARKO and WT mice in the presence of 10 nM $1\alpha,25(OH)_2D_3$. (*b*) Pit area resorbed by osteoclasts over an additional 48-h period of coculture on a dentine slice. (*c*) Osteoclast formation in cultured M-CSF-dependent bone marrow macrophages. (*d*) Survival rate of isolated osteoclasts formed during coculture of osteoblasts and bone marrow cells. (*e*) Gene expression of *RANKL* and *G3PDH* in cultured primary osteoblasts from male ARKO and WT littermates.

Fig. 5. Schema of skeletal sex hormone action. In male WT mice, skeletal sex hormone activities are mediated by both AR and ER. In female WT mice, skeletal function of ER is likely to dominate over that of AR as serum levels of AR ligands in females are quite low. In male ARKO mice, testicular testosterone production is severely impaired by hypoplasia of the testes, leading to a lack of skeletal sex hormone actions. In contrast, female ARKO mice may not be greatly affected by disruption of AR signaling.

Discussion

The present study, using orchidectomized ARKO mice, directly demonstrates that AR function is essential for androgen effects on the male skeleton. Although a number of previous studies have assessed the bone phenotypes of testicular feminization mutant rodents and humans eventually treated with sex hormones (3, 5), it has still been difficult to isolate AR functions in the skeletal system due to the local conversion of androgens to estrogens (6). When aromatizable testosterone (Fig. 3*e*) was given to orchidectomized ARKO mice, bone loss was only partially prevented, clearly establishing the pivotal function of AR in male-type bone remodeling. This finding is supported by previous reports concerning the beneficial effects of testosterone in male $ER\alpha^{-/-}$ and $ER\alpha\beta^{-/-}$ bone (22). As no clear bone loss in female ARKO mice was detected, AR is likely to be one of the determining factors in the formation of male-type bone, along with other AR downstream factors that may be encoded in male-specific Y chromosome regions. However, as bone loss was also induced by inactivation of either ERα or aromatase in male mice (23, 24), ER-mediated estrogen signaling also seems to be physiologically significant in the retention of male-type bone mass and bone remodeling. In such mice, high bone turnover with increased bone resorption was also observed. Therefore, it is possible that receptor-mediated signaling by both androgens and estrogens is convergent in the suppressive action on male bone resorption.

Unlike male ARKO mice, no overt differences in bone phenotype and mass were found between female AR-deficient and WT littermate mice at 8 weeks of age. Although the effects of anabolic androgens on bone have been documented in female rodents and humans, the physiological function of AR may not be significant because of the probably dominant role of ER function in female bones (Fig. 5), reflecting the high levels of serum estrogens in females. However, under certain conditions, such as estrogen deficiency in postmenopausal women (4), AR-mediated androgen effects may become physiologically significant in the protection against bone loss. This hypothesis will be tested using ovariectomized female ARKO mice in future studies.

The higher rate of bone resorption than formation with increased osteoclastogenesis observed in the $AR^{L-/Y}$ mice has been implied in previous reports (3, 5, 25). However, several recent reports (19, 26, 27) were inconsistent with our findings that osteoclast precursor cells were unaffected by AR deficiency in terms of cell survival and responsiveness to well characterized osteoclastogenesis inducers such as $1\alpha,25(OH)_2D_3$ and M-CSF (Fig. 4 *a–d*). Similar to AR, critical ERα functions in osteoclast precursor cells from ERα-deficient ($ER\alpha^{-/-}$) mice were not detected during *in vitro* osteoclastogenesis, and increased expression of the *RANKL* gene in osteoblast was also found (unpublished results). Together with previous findings of suppressive ERα effects on RANKL signaling (28), we speculate that the convergent functions of AR and ERα in male bone formation and remodeling are mediated through their suppressive functions on RANKL gene expression in osteoblasts. To test this hypothesis, identification of the negatively regulatory elements by receptors in the *RANKL* gene promoter (29) is clearly required.

We thank Dr. Yoshiaki Azuma and the hard tissue research team at Kureha Chemical for technical assistance and Dr. Toru Akune for helpful discussion. This work was supported in part by grants-in-aid from the Ministry of Education, Science, Sports and Culture of Japan (to S.K. for priority areas and to H. Kawano).

1. Bland, R. (2000) *Clin. Sci.* **98,** 217–240.
2. Compston, J. E. (2001) *Physiol. Rev.* **81,** 419–447.
3. Bilezikian, J. P. (2002) *J. Bone Miner. Res.* **17,** 563–566.
4. Riggs, B. L., Khosla, S. & Melton, L. J., III (2002) *Endocr. Rev.* **23,** 279–302.
5. Hofbauer, L. C. & Khosla, S. (1999) *Eur. J. Endocrinol.* **140,** 271–286.
6. Simpson, E. R. & Davis, S. R. (2000) *Proc. Natl. Acad. Sci. USA* **97,** 14038–14040.
7. Couse, J. F. & Korach, K. S. (1999) *Endocr. Rev.* **20,** 358–417.
8. Takeyama, K., Ito, S., Yamamoto, A., Tanimoto, H., Furutani, T., Kanuka, H., Miura, M., Tabata, T. & Kato, S. (2002) *Neuron* **35,** 855–864.
9. Mangelsdorf, D. J., Thummel, C., Beato, M., Herrlich, P., Schutz, G., Umesono, K., Blumberg, B., Kastner, P., Mark, M., Chambon, P., *et al.* (1995) *Cell* **83,** 835–839.
10. Wilson, J. D. (1999) *Endocr. Rev.* **20,** 726–737.
11. McKenna, N. J. & O'Malley, B. W. (2002) *Cell* **108,** 465–474.
12. Glass, C. K. & Rosenfeld, M. G. (2000) *Genes Dev.* **14,** 121–141.
13. Yanagisawa, J., Kitagawa, H., Yanagida, M., Wada, O., Ogawa, S., Nakagomi, M., Oishi, H., Yamamoto, Y., Nagasawa, H., McMahon, S. B., *et al.* (2002) *Mol. Cell* **9,** 553–562.
14. Sato, T., Matsumoto, T., Yamada, T., Watanabe, T., Kawano, H. & Kato, S. (2003) *Biochem. Biophys. Res. Commun.* **300,** 167–171.